



CrossMark
click for updates

Cite this: *Catal. Sci. Technol.*, 2016, 6, 1265

Received 28th August 2015,
Accepted 13th January 2016

DOI: 10.1039/c5cy01437a

www.rsc.org/catalysis

Metal-supported carbon-based materials: opportunities and challenges in the synthesis of valuable products

E. Pérez-Mayoral,^{*a} V. Calvino-Casilda^a and E. Soriano^{*b}

Carbon materials such as activated carbons and graphitic materials and nanomaterials have been used for decades in heterogeneous catalysis as catalyst supports. The physical and chemical properties of these materials, such as their tunable porosity and surface chemistry, allow the anchoring and dispersion of the active phases, and make them suitable for application in many catalytic green processes. In this review, we summarize relevant applications and limitations of metal-supported carbons and nanocarbons in the synthesis of valuable products and the recent advances in this field.

1. Introduction

Traditional heterogeneous catalysts often exhibit relatively low activities because of the limited accessibility of the reagents to the catalytically active sites. This drawback can be overcome by supporting the active phases on other porous in-

organic solids such as silica, zeolite and mesoporous materials, among others. Therefore, the selection of the appropriate support is a topic of main importance.

For a long time, carbon-based materials have been found to be useful materials in catalysis as catalysts or even as supports of catalysts.¹ Among the advantages of these carbon-based materials for catalytic applications are their i) high chemical stability in acid or basic media, ii) low corrosion capability, iii) high thermal stability, iv) hydrophobic character, v) easy recovery from the reaction mixture and, vi) from the economic point of view, their lower price. In fact, some

^a *Departamento de Química Inorgánica y Química Técnica, Universidad Nacional de Educación a Distancia, UNED, Paseo Senda del Rey 9, E-28040 Madrid, Spain. E-mail: eperez@ccia.uned.es*

^b *Instituto de Química Orgánica General, CSIC, C/Juan de la Cierva 3, E-28006 Madrid, Spain. E-mail: esoriano@iqog.csic.es*



E. Pérez-Mayoral

Elena Pérez Mayoral studied Chemical Sciences at the Complutense University of Madrid (UCM, Spain) where she obtained her Ph.D. in 1999 concerning organic photochemistry. After a post-doctoral stay at the National Distance Education University (UNED) and at the J. Heyrovsky Institute of Physical Chemistry (the Academy of Sciences of the Czech Republic, Prague), she became an Assistant Professor at the UNED

in 2011. She has worked in different research fields, including medicinal chemistry, on the synthesis of cyclin-dependent kinase inhibitors and on the design of lanthanide complexes as contrast agents for magnetic resonance imaging (MRI). Her current research interests are focused on the design of new nanocatalysts involved in the synthesis of biologically relevant heterocyclic systems and related compounds.



V. Calvino-Casilda

Vanesa Calvino-Casilda obtained her Ph.D. degree at the UNED (Madrid, Spain) in 2008 under the supervision of Prof. Rosa M^a Martín-Aranda and Prof. Antonio J. López-Peinado. Later, she worked in the Catalytic Spectroscopy Laboratory as a postdoctoral researcher at the Institute of Catalysis and Petrochemistry (CSIC, Madrid) under the supervision of Prof. Miguel A. Bañares (2008–2013). Since 2014, she has worked at the Faculty of Science (UNED, Madrid) as a postdoctoral researcher/teaching staff. Her research focuses on the intensification of heterogeneous catalytic processes for fine chemical synthesis and real-time Raman reaction monitoring.

in 2014, she has worked at the Faculty of Science (UNED, Madrid) as a postdoctoral researcher/teaching staff. Her research focuses on the intensification of heterogeneous catalytic processes for fine chemical synthesis and real-time Raman reaction monitoring.

carbon materials stand out for their industrial applications as adsorbents² and especially in fine chemical production.³

Generally, the carbon materials with catalytic applications have a graphitic structure, where the π -electron system of the basal planes is responsible for the basicity of these materials.⁴ Furthermore, the concentration and nature of the organic functional groups, bearing different heteroatoms (mainly O, N, H, Cl, S), over the surface of the carbon, contribute to the changes in their acid–base character and redox properties (Fig. 1), thus affecting their textural properties to a greater or lesser extent, and playing a crucial role in their catalytic behaviour.

The oxygenated groups are the most extensively investigated functionalities due to the fact that the oxygen combined with the carbon atoms forms a wide variety of organic acid and base functionalities. It is well known that these functionalities are easily formed during the synthesis or by oxidant post-treatment of the corresponding carbon material and, even, by exposure of the material to the atmosphere itself.⁵ While the carboxylic acids and anhydrides, lactones or lactols, and phenols exhibit an acid character, the carbonyl and ether groups are considered neutral functionalities. Other organic oxygenated functionalities, such as quinone, chromene and pyrone are proposed, although without consensus, as basic oxygen-containing functionalities which might be involved in surface redox processes.

In this sense, the quantum chemical calculations reported by Fuente *et al.*⁶ concerning the pyrone-like model compounds suggest that these organic functional groups are relevant for carbon basicity. The calculated pK_a values for these functionalities, in the range of 4–13, depend on the relative position of the ketone and etheric rings.

Many types of carbon materials have been used to prepare carbon-supported catalysts, such as carbon black, activated carbon (AC), glassy carbon, pyrolytic carbon and polymer-derived carbon. Among them, the ACs and carbon black are

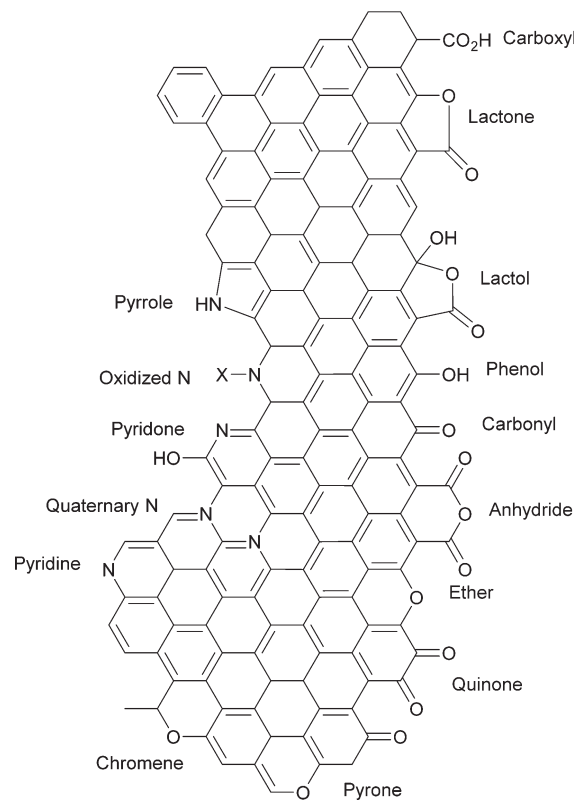


Fig. 1 Organic functional groups on carbon materials.

the carbon-based materials most frequently used as the supports of the active phases, mainly due to their high surface areas.⁷

Carbon is, then, considered an old⁸ but also a new catalytic material. In the past decades, the development of new nanocarbons, also known as nano-structured carbon materials, including the modification and functionalization of the different carbon allotrope structures with interesting applications, has undergone spectacular progress (Fig. 2).⁹

Nowadays, three different nanocarbon generations with catalytic applications are recognized: i) the 1st generation,



E. Soriano

Elena Soriano obtained her Ph. D. degree in 2003 at the UNED (Madrid). She was a postdoctoral fellow of Gobierno de La Rioja (2005–2006) and MEC (Juan de la Cierva contract, 2006–2008) working at the IIB “Alberto Sols” (UAM-CSIC). In 2008, she was granted a Tenured Scientist position in the Spanish Council for Scientific Research (CSIC) at the Instituto de Química Orgánica General (Madrid), and in 2015 she has

been promoted to Senior Researcher Scientist. Her research interests focus on the application of computational tools to the study of reaction mechanisms (mainly processes catalyzed by transition metals and organocatalysis) and drug design.

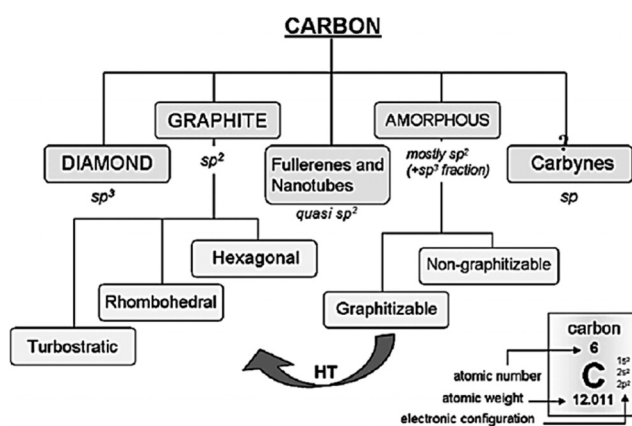


Fig. 2 Allotropes of carbon. Reprinted with permission from ref. 9. Copyright © 2007 Wiley-VCH.

characterized by low dimensionality and morphology-defined properties, such as fullerene (zero dimension), CNTs (one dimension), graphene (two dimensions) and mesoporous carbons (three dimensions) and their derivatives; ii) the 2nd generation, in which heteroatoms are introduced; and iii) the 3rd generation, including the designing of hybrid and/or hierarchical systems.

Depending on the preparation and functionalization, nanocarbons can show a rich functional surface activity, with different types of surface groups, showing themselves a rich catalytic chemistry. Thus, the electronic structure is tailored by introducing heteroatoms, their physical properties are tuned by controlling the pore structures, and their chemical properties are changed by specific surface functional groups. In other words, a level of control in the characteristics of the nanocarbon is introduced during the synthesis or by post-synthesis treatments. In addition, a further level of control in the properties of nanocarbons can be reached by designing hybrid and/or hierarchical systems. These materials are nano-architected, *e.g.* the reactivity properties depend critically on the nano-architecture, not only in terms of mass transfer, the classical motivation to realize hierarchical structured catalysts.

The synthesis and application of carbon-supported catalysts have been the subject of several reviews.^{1a,10} However, the goal of this paper consists of an update addressed to review the applications of metal-supported carbons and nanocarbons, particularly in the synthesis of valuable products. This contribution pays special attention to the use of ACs as their unique properties make them one of the most preferred supports.

2. Activated carbons

ACs are the most studied carbon-based material as supports for noble metals. The high dispersion and stability of the metallic phases on ACs are possible mainly due to their large surface areas.^{5a} In some cases, the presence of functionalities over their surface is especially relevant for anchoring the metallic phases even as coordination complexes. Both the texture and surface chemistry of ACs influence the catalytic performance of AC supported catalysts. ACs are used commercially in many catalytic formulations, particularly for hydrogenation catalysts, for the excellent properties of dispersion of metal particles (particularly based on noble metals) and the absence or (limited) presence of sites, which may catalyse side reactions. In addition, they are less expensive compared to alumina and silica supports and the active phase can be recovered by eliminating the support through burning away the carbon. In the subsequent sections we review the types of metal-supported ACs involved in the catalytic processes of fine chemicals.

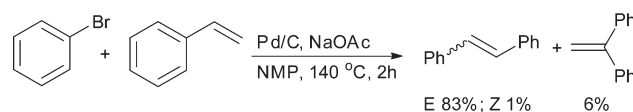
2.1 Metal supported ACs

Metal supported ACs have been used for a variety of chemical reactions, mainly C–C coupling reactions, hydrogenations, oxidations or carbonylations. The C–C bond forming reactions are fundamental and versatile transformations in synthetic

organic chemistry. Among them, the Heck C–C coupling reactions are of growing interest in the fine chemical industries. In 1972, Heck *et al.*¹¹ found that heterogeneous palladium catalysts supported on AC (Pd/C) could perform the substitution of vinyl derivatives with aryl halides, although with inferior yields to those obtained using homogeneous palladium catalysts. Later, it was demonstrated that there is a close correlation between the properties of the Pd/C catalysts and the reaction efficiency, and it depends mostly on the type of reaction.¹² One of the most critical parameters for the Pd/C catalysts is the palladium distribution. Thus, Pd/C catalysts are classified into “eggshell”, “thickshell” and “uniform”. In the case of the “eggshell” catalysts, palladium is distributed closely to the surface within 50–150 nm depths, whereas in the “thickshell” catalysts, palladium is distributed to depths of 200–500 nm from the surface. In contrast, palladium is dispersed homogeneously in the “uniform” catalyst. Arai *et al.*¹³ elucidated the mechanism of the palladium supported on AC catalyzed Heck coupling reaction. In the reaction of iodobenzene with methyl acrylate in the presence of Pd/C, triethylamine and sodium carbonate, at 160 °C, triethylamine seemed to reduce Pd(II) to Pd(0), while the role of sodium carbonate was to neutralize the acid formed during the reaction. On the other hand, the use of trimethylamine, besides sodium carbonate, led to a high rate acceleration and a major recovery of palladium. Moreover, the reaction seemed to take place when the colloidal palladium, which is obtained by partial aggregation of the dissolved palladium, was redissolved catalyzing again the reaction.

Köhler *et al.*¹⁴ found that oxidic uniform Pd/C catalysts with a high water content (55%) were active catalysts in the Heck coupling of bromobenzene with styrene, affording *trans*-stilbene in high yield and selectivity (Scheme 1). It seemed that the water content in the Pd/C catalysts accelerated the reaction, inhibiting the precipitation of the inorganic species on the surface of the metal. In addition, the palladium dissolved in the solution appeared to catalyse the reaction, increasing also its average size with the reaction time. Thus, the Pd/C catalysts changed their morphology from uniform to eggshell, with palladium deposited mostly on the surface of the support. Therefore, Pd leaching of heterogeneous catalysts was required for high activity and selectivity in the Heck reactions.¹⁵

Later, Fan *et al.*¹⁶ carried out the continuous multi-step synthesis of 1,2-diphenylethane in a structured compact multichannel reactor. The reaction involved a Heck C–C coupling reaction followed by the reduction (alkene hydrogenation) of the intermediate obtained (Scheme 2). Microspherical AC-supported Pd catalysts catalysed both steps. The flow

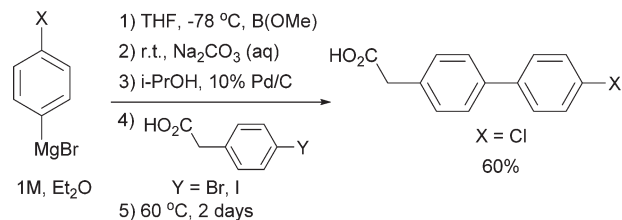


Scheme 1 Heck coupling reaction of bromobenzene with styrene over a Pd/C catalyst.

process in the compact reactor was more efficient than in the discontinuous reactor (batch). Thus, the reaction time was reduced significantly from hours to minutes, additional ligands were also not used, and the reaction was carried out under milder reaction conditions (lower values of pressure and temperature). The Pd leached in the Heck C–C coupling step was efficiently recovered in the following reduction step. In this manner, a reverse flow operation could normally retain the catalytic activity of the system demonstrating that a compact reactor was capable of carrying out the multi-step synthesis in only one stream.

The importance of developing carbon catalysts for use in Suzuki cross-coupling reactions with aryl chlorides has aroused great interest. Buchecker *et al.*¹⁷ carried out the Suzuki–Miyaura coupling of aryl bromide with aryl boronic acid, in the absence of phosphine ligands, using Pd/C heterogeneous catalysts. The procedure was only valid to aryl bromides and iodides but not for aryl chlorides because a significant degree of hydrodechlorination was observed. The authors performed some additional experiments with the Pd/C catalysts and concluded that under the reaction conditions used, the coupling reactions occurred by heterogeneous catalysis. In the literature, Pd(0) was always suggested to be active as a complexed homogeneous species in this type of reactions, however in this case the authors demonstrated, for the first time, that Pd(0) acted in a heterogeneous form. Then, Gala *et al.*¹⁸ showed, for the first time, that the carboxylic acid group is compatible with the Suzuki reaction. They accomplished the synthesis of a biphenylacetic acid derivative through coupling of an arylboronic acid (derived from a Grignard reagent) with bromophenylacetic acid over the Pd/C catalysts. The reaction procedure, without phosphine ligands and degassed solvents, afforded the coupling product in a good yield (Scheme 3). The process was also scaled up to a multikilogram preparation of 4'-fluorobiphenylacetic acid.

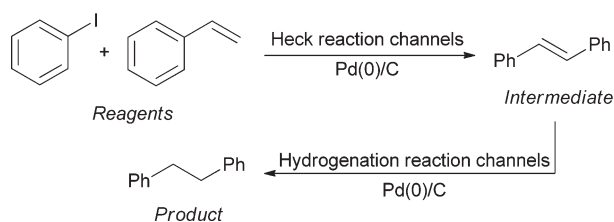
Sun *et al.*¹⁹ reported the Suzuki cross-coupling reaction with aryl chlorides over Pd/C catalysts without added ligands. It seems that both the tri-*tert*-butylphosphine and triphenylphosphine ligands poisoned the reaction. They suggested that a synergistic anchimeric and electronic effect that takes place between the Pd surface and the aryl chloride could explain the C–Cl bond activation. The selection of the suitable reaction medium was also crucial for this cross-coupling reaction. Then, El-Sayed *et al.*²⁰ compared the catalytic activity of carbon-supported spherical poly(*N*-vinyl-2-pyrrolidone) palladium (PVP-Pd) nanoparticles and colloidal



Scheme 3 Synthesis of a biphenylacetic acid derivative over a Pd/C catalyst.

spherical poly(*N*-vinyl-2-pyrrolidone) palladium nanoparticles in the Suzuki reaction between phenylboronic acid and iodobenzene to obtain biphenyls. The carbon-supported colloidal Pd nanoparticles showed higher activity during the first cycle of the reaction than the carbon-supported spherical Pd nanoparticles. However, after the second cycle, the carbon-supported Pd nanoparticles showed a recycling potential that is double that of the colloidal Pd nanoparticles. Moreover, the catalytic activity of the carbon-supported colloidal Pd nanoparticles decreases during the following second to fifth cycles of the Suzuki reaction while the catalytic activity of the carbon-supported Pd nanoparticles remains almost constant. It seemed that the particle size played a significant role. The carbon support protected the Pd nanoparticles during the reaction preventing aggregation and precipitation in contradistinction to the colloidal Pd nanoparticles. After these research studies, Köhler *et al.*²¹ exposed that hydrophobic surfaces, such as those shown by Pd/C, play an important role in the Suzuki coupling reactions in water showing high activity (Scheme 4). However, those catalysts with hydrophilic surfaces, like palladium on metal oxides, showed low activity for the Suzuki coupling reactions in water. In this case, these catalysts could improve their catalytic activity by tuning the surface polarity of the metal oxide supports or using stronger alkaline conditions (adding an excess of base). The hydrophobic surface of the Pd/C catalysts with better catalyst dispersion in the phase containing organic substrates might cause enrichment of the substrate at the catalytic surface. The supported Pd in contact with the substrate was responsible for the formation of the active species that resulted in higher conversions. It seemed that the reaction occurred near the catalyst surface, within a droplet or layer of the catalyst substrate.

The exclusive homogeneous or heterogeneous catalysis of the Suzuki reaction seems to be inconsistent as anticipated; some authors suggest then the possibility of the “soluble” Pd



Scheme 2 Synthesis of 1,2-diphenylethane over a Pd/C catalyst.



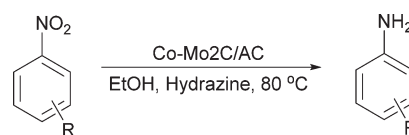
Scheme 4 Suzuki coupling reaction of 4'-chloroacetophenone catalyzed by Pd/C or Pd/Al₂O₃ in water.

nanoparticle formation after Pd leaching from the surface of the supported catalysts. To this end, Kçhler *et al.*²² reported a highly active and robust heterogeneous Pd-based catalyst (Pd/C, Pd/metal oxides and Pd/zeolite) for the Suzuki reactions leading to the corresponding biaryls with total selectivity without exception, in quantitative yields and with short reaction times. The catalysts were reusable several times by the addition of iodine as an oxidizing agent. The authors concluded that the Pd concentration in solution during the reaction correlates clearly with the progress of the reaction (conversion) indicating that the dissolved molecular Pd is the catalytically active species; after the end of the reaction, the dissolved Pd is deposited onto the support.

Hermans *et al.*²³ prepared palladium carbon (Pd/C) supported catalysts using precursors of grafting carboxylate on functionalized carbon. The carbon supports were functionalized by treatment with HNO₃ and H₂O₂, and the corresponding oxygenated functionalities formed were used as anchors for the Pd precursors, Pd carboxylate complexes (Pd(O₂CR)₂(N-ligand)_x), by covalent bonding. The Pd/C catalysts were used in the 2-methyl-2-nitropropane hydrogenation to obtain *t*-butylamine. Apparently, there was a correlation between the catalytic activity and both the initial carbon acidity and Pd dispersion, in the case of the HNO₃-modified samples. This was not the case for the H₂O₂-modified samples, probably due to the presence of different types of oxygenated surface groups. They served as anchors for the Pd precursors playing an important role during the catalytic process. Then, Okhlopkova²⁴ studied the influence of the acidity of the solution on the dispersion of platinum supported on an AC catalyst and its activity in the hydrogenation of cyclohexene. An acidic solution indeed influenced the platinum dispersion, decreasing the activity of Pt/C in the cyclohexene hydrogenation when the dispersion is increased. This fact was due to the localization of the metal species in the narrow pores of the support blocking the access of reagents. This effect seemed to be larger on those supports containing smaller pores and a higher concentration of the oxygen functional groups. Later, Davis *et al.*²⁵ reported supported bimetallic Pt–Re nanoparticles on Norit AC for the glycerol hydrogenolysis reaction. The bimetallic Pt–Re clusters on AC were more active than either monometallic Pt or Re. Catalysts containing Re could only be reduced under hydrogen when coexisting with Pt, apparently by spillover dissociated hydrogen atoms from Pt to Re. The Pt–Re/C catalyst achieved a better catalytic performance when sintered at high temperatures, enhancing the atomic mixing of Pt and Re and not decreasing considerably the metal dispersion. More recently, Kaprieloba *et al.*²⁶ prepared Pt/C catalysts by reductive deposition in the aqueous phase. The AC support worked as an effective nucleating agent and ensured the formation of small Pt particles avoiding the formation of aggregated Pt particles. This fact was probably due to the oxide nucleus formation on the AC surface. The high deposition rate provides Pt nanoparticles in the narrow pores and outside of the micropores (eggshell Pt distribution). Thus, the catalytic properties could be

affected by the support, the platinum loading and the conditions used during the deposition, keeping the same metal precursor. The Pt/C catalysts were active in the isopropyl alcohol oxidation probe reaction showing an almost total alcohol conversion and a TOF of 80 000 h⁻¹.

Halttunen *et al.*²⁷ explored the stability of Rh and Ru catalysts supported on AC in the hydrocarbonylation of methanol in the liquid phase. The metal dispersion was related to the stability of the Rh-supported catalysts, with the stability worse when the dispersion was higher. The catalytic activity showed by the Rh supported on AC catalysts was related to the amount of metal leached from the support. They concluded that these heterogeneous catalysts were not appropriate for the methanol hydrocarbonylation in the liquid phase but they could be in the gaseous phase. Then, Wettstein *et al.*²⁸ prepared RuSn supported on AC as catalysts varying the tin content for the levulinic acid hydrogenation to γ -valerolactone. The addition of Sn to the Ru/C catalysts significantly influenced the catalytic properties, improving the selectivity and stability in the studied reaction. The catalyst containing only Ru was the most active catalyst but underwent deactivation with the time on stream. However, the catalyst containing the same amounts of Ru and Sn showed a lower activity but improved stability and selectivity with the time on stream. Increasing the Sn content triggered the formation of an additional phase (β -Sn) that was not active under the reaction conditions. From all the RuSn supported on AC catalysts prepared, the RuSn₄/C catalyst was the most active and stable catalyst to produce γ -valerolactone. Recently, Zhao *et al.*²⁹ carried out the chemoselective reduction of different substituted nitroarenes to obtain different functionalized arylamines using supported Co-promoted Mo carbide catalysts on modified AC (Co–Mo₂C/AC) (Scheme 5). The addition of a small amount of a transition metal such as Co seemed to promote considerably the formation of the molybdenum carbide crystal phase. This resulted in an improvement in the catalytic activity of the supported molybdenum carbide catalyst due to a synergistic effect, affording a total conversion and selectivity in all the cases. The Co–Mo₂C/AC catalyst could be considered for industrial applications related to the production of functionalized arylamines. Lately, Gallegos-Suárez *et al.*³⁰ supported Ru on different carbon materials (AC, graphite and multi-walled carbon nanotubes) for use as catalysts (Ru/AC, Ru/HSAG and Ru/CNT) in the hydrogenolysis of glycerol in the liquid phase. The CO microcalorimetry results showed that the graphite and carbon nanotube supports possess electron donor properties capable of



Scheme 5 Chemoselective reduction of various substituted nitroarenes to the corresponding functionalized arylamines over the developed supported metal carbide catalysts on AC.

promoting the formation of an electron-rich metal species ($\text{Ru}^{\delta-}$). Thus, Ru supported on graphite and carbon nanotube catalysts promote 1,2-propanediol formation from glycerol, and improve the consecutive C–C cleavage forming undesired products, such as methane ($\text{Ru}/\text{CNT} > \text{RuHSAG}$). On the other hand, Ru supported on AC showed ethylene glycol as the main product in the conversion of glycerol on the metal sites.

Kim *et al.*³¹ studied palladium and copper supported on AC catalysts for the oxidative carbonylation of phenol and bisphenol-A to obtain diphenyl carbonate or polycarbonate oligomers used as intermediates in the phosgene-free polycarbonate synthesis. Metallic Pd with some fraction of its surface oxidized, and cuprous oxide were the initial states of Pd and Cu when they were supported on AC. However, the metallic character of Pd was enhanced during the oxidative carbonylation and the Pd–Pd coordination number increased to almost twice. In the case of the copper supported on AC catalyst, cuprous oxide (initial state) was converted into a rare linear cuprous dibromide complex that was stabilized by a tetrabutylammonium cation. The cuprous complex seemed to be the active key catalytic component to obtain the desired aromatic carbonates. On the other hand, the role of the carbon-supported metallic Pd catalyst in the oxidative carbonylation of phenols was the oxidative regeneration of hydroquinone to benzoquinone with the production of water as the by-product. This research group also studied the coupled oxidative carbonylation of bisphenol-A and phenol using Pd/C catalysts and different metal complexes of Ce, Co, Mn and Cu as inorganic co-catalysts (Scheme 6).³² The heterogeneous catalytic system formed by Pd supported on AC and Cu_2O as a co-catalyst showed improved catalytic properties with better activity and selectivity results than the Pd homogeneous system. The active phase of the Pd/AC– Cu_2O – Bu_4NBr –BQ catalytic system was established by the metallic Pd particles with the catalytic performance independent of the Pd initial state in Pd/AC as was evidenced by the Pd K-edge EXAFS studies.

2.2 Metal oxide supported ACs

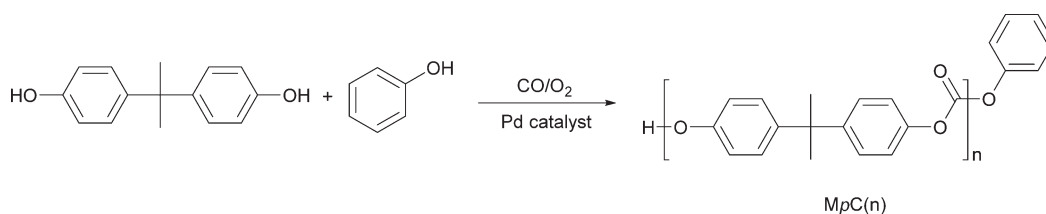
Metal oxide supported AC catalysts have been successfully used for a great variety of chemical reactions, such as oxidations, reductions, transesterifications, or alkylations, among others. Selective oxidation of alcohols into the corresponding aldehydes/ketones is a transformation extremely useful in organic synthesis (Scheme 7). The carbonyl components are involved in the production of plastic, dyestuff, perfume, flavor

and pharmaceuticals, among other applications.³³ This process often requires the use of stoichiometric amounts of highly contaminant inorganic oxidants such as chromium(vi) salts. Therefore, the development of new methodologies with reduced environmental impact using clean oxidants, H_2O_2 , or even operating under aerobic conditions is a challenge of prime importance.

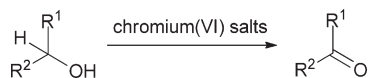
In this sense, manganese oxide and vanadium oxide-supported AC catalysts have been reported by Chen *et al.*³⁴ for the aerobic and selective oxidation of benzyl alcohol to benzaldehyde. An enhancement of the catalytic activity (from 31 to 67% when using Mn/C -0.5 M HNO_3 and from 46 to 93% for V/C - O_2 for 3 h) was observed when the metal oxides were supported using the previously oxidized AC support. It is probably due to the presence of the specific variety and the increased density of the oxygen-containing complexes on the AC support surfaces. The ACs under study showed similar particle dispersion and the metallic centers maintained the oxidation state and coordination environment before and after oxidant pretreating of the AC support.

Zhu *et al.*³⁵ reported a cheap, effective and reusable $\text{Co}_3\text{O}_4/\text{AC}$ catalyst, working in the absence of any promoter, for benzyl alcohol oxidation, in the presence of molecular oxygen under mild conditions. Among the metal oxides investigated by the authors, Co and Ni oxide supported ACs were the most promising catalysts for the aerobic oxidation of benzyl alcohol, whereas other metal oxides such as the Mn, Fe, and Cu ones exhibited lower conversion and selectivity. $\text{Co}_3\text{O}_4/\text{ACs}$ were prepared by a wet impregnation method and subsequently first dried in an air oven at 110 °C overnight and then treated in N_2 or Ar at 350 °C. Quantitative conversion of the alcohol was obtained when using the samples treated under an Ar atmosphere. It is noteworthy that these catalysts can be reused without any significant activity loss. The authors proposed a plausible reaction mechanism for this transformation consisting of two fundamental steps: i) the molecular oxygen activation occurring by adsorption on the defects on the carbon support, and ii) the alcohol dehydrogenation taking place over Co_3O_4 . The high catalytic activity observed for the cobalt-supported ACs was comparable to the other noble metal-supported AC catalysts, such as Au/AC.

The epoxidation of olefins plays an important role in the industrial production of fine chemicals. Particularly, ethylene oxide and its derivatives are extensively used for multiple applications in the production of electronics, pharmaceuticals, pesticides, detergents, among others.³⁶ In this regard, a well-



Scheme 6 Synthesis of mono phenylcarbonate-ended oligomers (denoted as MpC(n)) over palladium catalysts.



Scheme 7 Oxidation of alcohols into the corresponding carbonyl compounds.

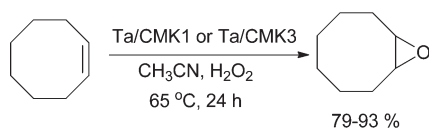
dispersed tantalum oxide on an ordered mesoporous carbon (CMK-3 or CMK-1) catalyst tested in the epoxidation of cyclooctene, in the presence of aqueous H_2O_2 , has been reported by Lin *et al.* (Scheme 8).³⁷

CMK-3 and CMK-1, as carbon replicas of the mesoporous silicas SBA-15 and MCM-48, respectively, exhibited higher catalytic performance, excellent selectivity and recyclability than tantalum oxide supported on AC and also over mesoporous silica SBA-15. While all of the investigated catalysts supported on carbon showed high epoxide selectivities (around 85%), the use of the tantalum oxide supported on SBA-15 catalyst afforded the corresponding epoxide with a lower selectivity (65%). This catalytic behavior could be attributed to the use of carbon supporting metal oxides that provide an adequate hydrophobic environment for the catalytic sites, thus facilitating the adsorption of olefins for selective epoxidation.

Metal oxide supported ACs have been also reported for interesting reduction reactions, such as the synthesis of anilines from nitro arenes or dehydrogenation of alkyl benzenes. It is important to note that anilines are key intermediates for the synthesis of pharmaceuticals, herbicides, polymers, and other fine chemicals. Fluoroanilines (FA) are particularly important building blocks involved in the synthesis of a great variety of biochemical products.³⁸ The industrial production of anilines from nitroaromatics often is carried out in the presence of Pd/C catalysts, which exhibit a high intrinsic activity but also low selectivity to the desired product.

Zhao *et al.*³⁹ synthesized and characterized a novel highly selective and active carbon-supported Pd/SnO₂ catalyst for the hydrogenation reaction of 2,4-difluoronitrobenzene (DFNB) to the corresponding 2,4-difluoroaniline (DFAN) in the presence of ethanol. The Pd/SnO₂/C catalysts were prepared by first deposition of the SnO₂ onto the carbon support, followed by the deposition of Pd. The notable synergistic effect of the Pd and SnO₂ nanoparticles and significant performance and selectivity enhancements (Table 1) were reported. These results are probably because of the coordination action between the NH₂ groups and the Sn²⁺ or Sn⁴⁺ species at the surface of SnO₂, produced under a H₂ reductive atmosphere, forming Pd–Snⁿ⁺ ion pairs.

One of the other most important basic chemicals in the petrochemical industry is styrene (ST). It is industrially



Scheme 8 Epoxidation of cyclooctene, in the presence of aqueous H_2O_2 , catalyzed by supported tantalum oxide.

produced from ethylbenzene (EB) by dehydrogenation using $\alpha\text{-Fe}_2\text{O}_3\text{-K}_2\text{CO}_3$. Several researchers have reported the effect of using different porous catalytic systems in the presence or absence of CO_2 as an alternative diluent. However, the traditional catalyst above mentioned used for ST production did not exhibit significant catalytic activity when using CO_2 (yield to ST 1.9%). In this respect, Sugino *et al.*⁴⁰ reported the dehydrogenation of EB catalyzed by a different series of carbon-supported iron catalysts. These catalysts were prepared by impregnating a carbon support with aqueous solutions of iron nitrate. In the case of the carbon-supported iron catalysts co-loaded with an alkali metal and an alkaline earth metal, they were prepared by either successive impregnation of a carbon support with solutions of an iron nitrate and alkali metal or alkaline earth metal nitrates, or by co-impregnation using solutions containing both salts. The investigated carbon-supported iron catalysts afforded a high ST yield (up to 50%) in the presence of excess CO_2 . The increased loading of lithium nitrate (0.1 to 0.3 mol to 1 mol of the iron catalyst) particularly resulted in a significant increase in the catalytic activity. In this case, under pretreatment of the catalyst with CO_2 , at 973 K, iron and lithium on the carbon surface were converted into magnetite and lithium ferrite. Then, it seems that the lithium ferrite phase was found to be the active phase in the reaction of EB to ST. The authors proposed the following redox catalytic cycle: i) the lattice oxygen of iron oxide in lithium ferrite abstracts the hydrogen from EB to give ST and ii) CO_2 oxidizes the oxygen defects in the iron oxide phase in lithium ferrite.

In a similar way, Saito *et al.*⁴¹ described the role of lattice oxygen in V, Cr, and Fe oxide-loaded catalysts in the dehydrogenation of EB applying a transient response technique, an efficient method for analyzing the performance in an unsteady state catalytic reaction. As in the other cases, the catalysts were prepared by impregnation of the support with an aqueous solution of the corresponding metallic salts and subsequent calcination at different temperatures depending on the used support. The best catalytic results were found for the dehydrogenation process catalyzed by the V, Cr, and Fe oxide/AC catalysts. In order to study the promoting effect of CO_2 , the reaction was carried out using a fixed bed flow type quartz reactor operating at atmospheric pressure and the dehydrogenation of EB was carried out under Ar and CO_2 atmospheres. While in the presence of Ar, the lattice oxygen of the

Table 1 Hydrogenation of DFNB promoted by Pd catalysts^a

Catalyst	Conversion (%)	Selectivity ^b (%)	Reaction rate ^c
Pd/C	100	96.47	1.99
Pd/SnO ₂	100	99.96	0.84
Pd/SnO ₂ /C	100	100	3.72

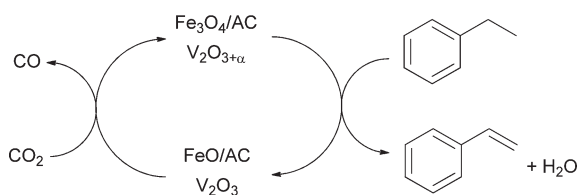
^a Reaction conditions: 0.1 g of catalyst, 20.0 g of DFNB, 15 mL of EtOH, P_{H_2} = 1.0 MPa, T = 353 K, stirring rate = 1000 rpm. ^b Only aminodiphenylamine and nitrodiphenylamine were detected among the other by-products. ^c Expressed in mol of substrates per mol of Pd.

vanadium and iron oxides was transferred to EB at the beginning of the reaction; under CO₂, the transferred lattice oxygen was supplied partially from CO₂ to keep the vanadium or iron oxides as higher valence state oxides. The plausible mechanism for the dehydrogenation of EB over V, and Fe oxide/AC, under CO₂, is summarized in Scheme 9. In contrast, when using the Cr₂O₃-loaded catalysts, no significant oxygen transfer from the lattice oxygen of Cr₂O₃ to EB was observed and, hence, no promoting effect of CO₂ was observed.

Biodiesel fuel prepared from renewable sources is considered as an alternative to diesel fuel. It is produced by the transesterification reaction of triglycerides from oils and fats with low-molecular-weight alcohols; CaO exhibits high activity for this transformation. However, the main disadvantage of using CaO as a catalyst in the biodiesel production is the formation of the CaO-glycerin complex⁴² acting then as a homogeneous catalyst. To overcome this drawback, Zu *et al.*⁴³ selected different porous carbon materials, such as carbon molecular sieves, AC, and the nanoporous carbons NC-2 and CMK-3, as supports in the synthesis of active and stable CaO-based catalysts for the transesterification of triacetin with methanol. Among the investigated supports, NC-2 with mesoporous and/or microporous characteristics, showed very high activity, stability, and recyclability.

In the same way, carbon-supported MgO nanocomposites based on the NC-2 carbon material were investigated in the synthesis of ethyl methyl carbonate (EMC) prepared by the transesterification reaction of dimethyl carbonate (DMC) with diethyl carbonate (DEC).⁴⁴ It was observed that MgO/NC-2 with different MgO loadings (1.6 to 20 wt%) exhibited a remarkably higher transesterification activity than the other carbon-supported MgO catalysts. The presence of a high concentration of oxygen functionalities over the surface of the NC-2 support probably favored the high dispersion of the MgO particles. In this case, MgO/NC-2 showed high stability against leaching of the active species under the test reaction conditions, indicating the truly heterogeneous nature of this catalyst.

Some members of our research group reported MgO-supporting carbon materials, PET/MAG, for the synthesis of relevant nitrogen heterocyclic compounds, as a highly efficient sustainable alternative to the amino-grafted and bifunctional mesoporous silicas.⁴⁵ These hybrid basic materials, containing different MgO loadings, were synthesized by thermal calcination of homogeneous mixtures of poly(ethylene terephthalate) and magnesite, both as carbon and MgO



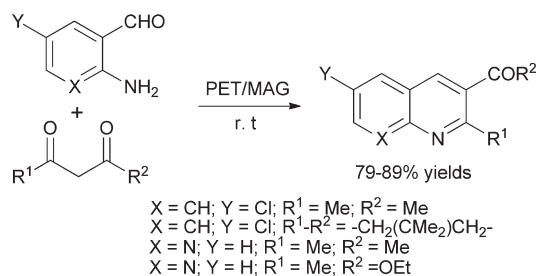
Scheme 9 Proposed reaction courses for the dehydrogenation of EB to ST under CO₂.

precursors, respectively. The combined materials are rich in MgO and revealed a bimodal, microporous–mesoporous character. These materials were investigated in the Friedländer condensation⁴⁶ of 2-amino-5-chloro-benzaldehyde and acetylacetone (R¹ = R² = Me), under solvent-free and mild conditions, affording the corresponding quinoline in good to excellent yields (up to 76%) with total regioselectivity (Scheme 10). The results reported demonstrated that MgO is the main catalytically active species. The activity of the catalysts apparently did not correspond to the MgO loading, but depended on the available catalytically active surface of the MgO crystals on the hybrid materials.

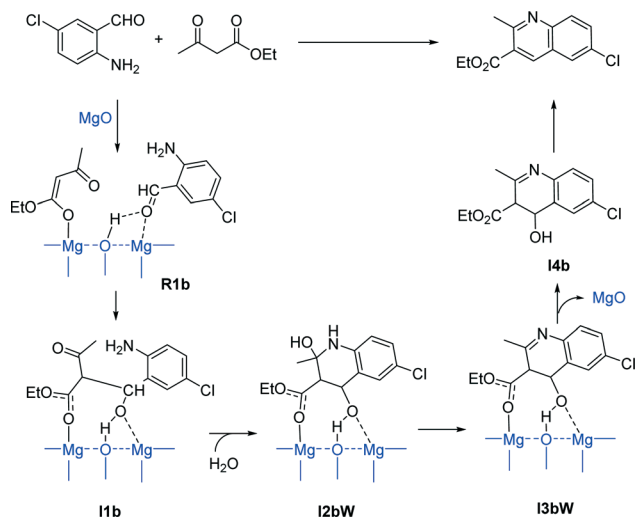
The scope of the methodology was demonstrated by reacting different 2-aminoaryl aldehydes and also different 1,3-dicarbonyl compounds leading to the corresponding biologically active heterocyclic compounds, such as naphthyridines and acridones.

On the basis of the DFT calculations, a reaction mechanism was postulated.⁴⁵ This analysis suggested a dual activation by the catalyst, as both carbonyl compounds are activated for the condensation (Scheme 11).

Carbon is known as a very efficient absorber of microwave (MW) energy as it effectively transforms the energy into heat. In this context, the use of alkaline carbons such as alkaline metal oxides supported over Norit carbon has been widely explored in our research group by combining alternative energy sources (MW and ultrasound). Thus, basic carbons are able to catalyze selectively the *N*-alkylation of imidazole with propargyl bromide, under MW irradiation.⁴⁷ The activity of the catalysts increased with the irradiation power, yielding *N*-propargyl imidazole in the highest conversion values when using Cs⁺-Norit carbon (an almost quantitative yield, with 100% selectivity, in 3 min of reaction time). In addition, the selective *N*-alkylation of imidazole and 2-methylimidazole with long-chain and medium-chain alkyl bromides, yielding imidazole derivatives exhibiting valuable pharmacological properties, such as antiparasitic, antifungal, and antimicrobial, was also reported (Scheme 12).⁴⁸ The *N*-alkylation of benzimidazole was also effectively performed, under MW activation, over basic carbon catalysts selectively yielding the corresponding alkylated heterocyclic compound in a high yield in very short reaction times (75% in only 5 min of reaction time).⁴⁹ Furthermore, the imidazole alkylation reaction, under ultrasound activation, was also investigated by some of



Scheme 10 Friedländer condensation of 2-amino-benzaldehydes and 1,3-dicarbonyl compounds.



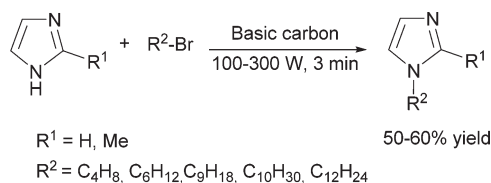
Scheme 11 Postulated reaction mechanism on the basis of DFT calculations.

us.⁵⁰ Thus, for the reaction between imidazole and 1-bromobutane promoted by alkaline carbons, an enhancement effect in the yield of the alkylated imidazole was observed.

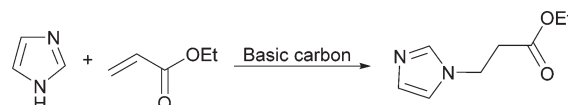
Another method, the real-time Raman monitoring of imidazole alkylation and the Michael addition reaction between imidazole and ethyl acrylate, promoted by these basic carbon and other acidic catalysts, has been also reported (Scheme 13).⁵¹ This non-invasive methodology provides molecular information on the reaction mechanism and possible species as intermediates of the reaction.

Following the alkylation reaction of heterocyclic compounds, Calvino-Casilda *et al.*⁵² reported for the first time an efficient and eco-friendly alternative for the preparation of *N*-substituted- γ -lactams promoted by alkali-loaded catalysts, Na-Norit, Cs-Norit and the bimetallic NaCs-Norit, under solvent-free conditions and MW irradiation. The carbon-nitrogen coupling reaction takes place between 2-pyrrolidinone and 1-heptanal selectively affording the *N*-1-heptenyl-2-pyrrolidinone. A notable enhancing effect in the yield under MW irradiation was observed in comparison with the conventional thermal activation methods (~70% yield in only 5 min to ~50% after 1 h of reaction time) (Scheme 14).

These carbon catalysts were also used in the synthesis of chalcones, relevant intermediates in the synthesis of many pharmaceuticals, by Claisen-Schmidt condensation under ultrasound irradiation (up to 50% yield) (Scheme 15).⁵³



Scheme 12 *N*-Alkylation of imidazoles with long-chain and medium-chain alkyl halides.

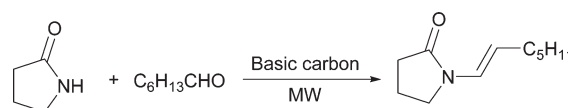


Scheme 13 Michael addition of imidazole and ethyl acrylate for the synthesis of *N*-substituted imidazole catalysed by basic carbon.

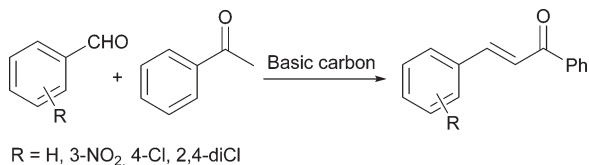
2.3 Immobilized coordination complex over ACs

Immobilized coordination complex over a solid support is a novel hybrid catalytic system able to merge the advantages of heterogeneous and homogeneous catalyses. This material has been used mainly in catalytic hydrogenation and oxidation reactions. The immobilization of the coordination complex over an AC support has received special attention due to the possibility of fine-tuning its textural properties and surface chemistry rich in oxygen functional groups. Palladium complexes containing aromatic ligands were the first coordination complexes immobilized over AC supports, whose catalytic activity was highly dependent on the location of the palladium center.⁵⁴ This study shows the importance of the metal complex position on the accessibility of the reactants to the active centers. Later, Bischoff *et al.*⁵⁵ prepared AC supported rhodium-phosphonate-phosphane catalysts for use in methanol carbonylation. They found that AC was a suitable support for hemilabile rhodium complexes but normal diffusion of reactants, at higher pressures, begins to limit the intrinsic high activity of the supported complexes. AC-heterogenized $[\text{PdCl}_2(\text{NH}_2(\text{CH}_2)_{12}\text{CH}_3)_2]$ catalysts were selective catalysts for the hydrogenation of 1-heptyne, where the support porosity played an important effect.⁵⁶ The position of the complex in the narrow pores induced shape selectivity due to the slit-shaped pores whereas ACs with a wider pore size distribution showed a negative effect in selectivity. The study was extended to other metal complexes with similar long-chain amine ligands. The authors proved that the anchored rhodium complex $[\text{RhCl}(\text{NH}_2(\text{CH}_2)_{12}\text{CH}_3)_3]$ supported on AC is an active and selective catalyst in the semi-hydrogenation of 1-heptyne.⁵⁷ The coordination compound was stable under the reaction conditions and was firmly attached to the AC support, constituting the active species of the catalyst.

Lemus-Yegres *et al.*⁵⁸ prepared the diamine Rh complex $[\text{Rh}(\text{COD})(\text{NH}_2(\text{CH}_2)_2\text{NH}(\text{CH}_2)_3\text{Si}(\text{OCH}_3)_3)]^+\text{BF}_4^-$ supported on AC catalysts for the hydrogenation of cyclohexene and carvone. For the first time, this research group exploited the phenolic surface groups of carbon materials for the immobilization of metal complexes through the creation of siloxane bonds (covalent bond) (Scheme 16). The active species were



Scheme 14 *N*-substitution of 2-pyrrolidinone with 1-heptanal under MW activation over basic carbon catalysts.

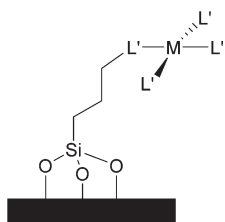


Scheme 15 Claisen-Schmidt condensation of substituted benzaldehydes and acetophenone.

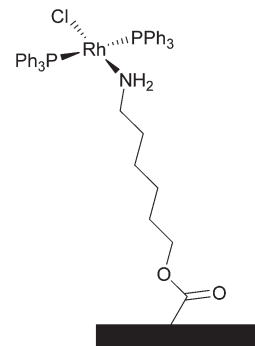
located inside the support porosity, where a minimum diameter of pores was required for the confinement of the metal complex. After this study, further research was extended using ACs oxidized in various ways (HNO₃, (NH₄)₂S₂O₈, and synthetic air) in order to obtain different surface chemistries.⁵⁹ The results showed that the catalysts with large amounts of oxygen groups hindered the location of the complex inside the porosity of the support, thus displaying a low catalytic activity. Then, this research group immobilized an Rh complex derived from the Wilkinson's catalyst on AC using an ester type covalent bond and a linear organic molecule (6-amino-1-hexanol) (Scheme 17).⁶⁰ This molecule acts as a linker and positions the complex away from the support surface to simulate its environment in the homogeneous phase. This catalyst was tested in the hydrogenation of cyclohexene resulting in a similar activity to the homogeneous Wilkinson's catalyst.

The catalyst CpTiCl₂(OC₆H₄Cl-*p*) was supported on three AC supports obtained from different precursors and subjected to ammoxidation in order to investigate the effect of the presence of nitrogen species.⁶¹ These catalysts were tested in the polymerization of ST showing that those catalysts modified by nitrogen species were less catalytically effective because the active centers were present only on the support surface and not in the pores.

Manganese(III) salen complexes have been demonstrated to be excellent catalysts in the epoxidation of unfunctionalized olefins, displaying high activity and enantioselectivity. Moreover, the hydroxyl groups, mainly the phenol type, present on the carbon surface or created by oxidation treatment, have been used to anchor the metal complexes. A Mn(III) Schiff base complex functionalized with hydroxyl groups on the aldehyde moieties [Mn(4-Hosalhd)CH₃COO] onto an AC showed that the oxidation of the support enhanced the catalyst adsorption whereas the acidity of the carbon surface had a negative effect on the ST



Scheme 16 Metal complex anchored on carbon supports through the siloxane bonds.



Scheme 17 Catalyst formed by a rhodium complex anchored on activated carbon.

epoxide chemoselectivities.⁶² These authors also immobilized a Schiff base nickel complex functionalized with hydroxyl groups, *N,N'*-ethylene-bis-(4-hydroxysalicyliminate)nickel(II), onto an AC using cyanuric chloride as the linking agent.⁶³ Then, they anchored chiral manganese(III) salen complexes on modified AC supports by direct axial coordination of the metal center onto the phenolate groups and tested them in the epoxidation of ST.⁶⁴ The modification of the AC was carried out by a reaction between sodium hydroxide and the surface phenol groups to obtain phenolate groups (CoxONa). They also studied the influence of the textural properties of four ACs on the immobilization process and on the catalytic performance of the Mn(III) catalysts.⁶⁵ Their results suggested that the total Mn(III) loadings increased with the pore size, as well as their distribution inside the carbon porous matrix.

Moura *et al.*⁶⁶ anchored iridium clusters over AC to use as heterogeneous catalysts in the selective hydrogenation of 1,5-cyclooctadiene. The formation of the fully hydrogenated product cyclooctane was observed when Ir metal supported on AC was used as a catalyst. However, when Ir₃ clusters were immobilized on ACs, these catalysts showed a special catalytic behaviour producing high activity and selectivity for the mono-hydrogenated product cyclooctene, and the isomerisation products 1,3-cyclooctadiene and 1,4-cyclooctadiene.

The current interest in transition metal complexes bearing tripodal capping C-scorpionate ligands, HC(pz)₃(Tpm), and their derivatives, is due to their diverse applications, such as in oxidation processes. Homogeneous and heterogenized Au(III) C-scorpionate complexes supported on carbonaceous materials (AC, carbon xerogel and carbon nanotubes) were used as catalysts for the single-pot peroxidative cyclohexane oxidation to cyclohexanol and cyclohexanone under mild conditions (H₂O₂ as an oxidant), at room temperature (Scheme 18).⁶⁷ The previous oxidation of the carbonaceous supports with HNO₃ or their oxidation with HNO₃ and subsequent treatment with NaOH led to the best heterogenization performance.

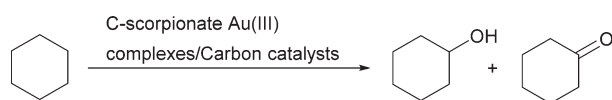
Recently, Silva and Botelho⁶⁸ immobilized Fe(II) and Fe(III) acetylacetonate onto amine functionalized ACs. The Fe complexes were anchored onto AC supports functionalized with (3-aminopropyl)triethoxysilane (APTES), through Schiff condensation of the carbonyl groups of the acetylacetonate

ligands and the APTES amine. The immobilized iron salts were active heterogeneous catalysts in the oxidation of cyclohexane and *n*-hexane with hydrogen peroxide at room temperature.

2.4 Heteropolyacid supported ACs

Catalysis based on heteropolyacids (HPAs) and their related compounds is an important field in which new and promising developments are being carried out both at the research and technological levels. Their highly acidic nature is very interesting in industrial reactions. Thus, they are used as an industrial catalyst in alcohol dehydration, alkylation or esterification reactions. In the past decades, HPAs have attracted great interest of catalyst researchers because their acid–base and redox properties are widely used in heterogeneous catalysis. HPAs are used as catalysts for organic synthesis processes in industries related to fine chemicals, such as the flavor, pharmaceutical and food industries. However, they are highly soluble in polar media and it is often difficult to separate them from the reaction media. Therefore, a new series of catalysts have been developed by supporting HPAs on various supports such as ACs. The impregnation of these supports with HPAs significantly increases their surface area, which is very important for heterogeneous catalysis processes. Izumi and Urabe were pioneers in supporting HPAs on ACs to be used as catalysts in the intermolecular dehydration of butanol and *t*-butyl alcohol in the liquid phase.⁶⁹ They proposed that there is no loss of the active component during the reaction proving that AC is an excellent carrier to entrap HPAs. Later, Chimienti *et al.*⁷⁰ prepared tungstophosphoric acid (TPA) and tungstosilicic acid (TSA) supported on AC catalysts by equilibrium and incipient wetness impregnation techniques and tested them in the dehydration of isopropanol. The samples prepared by the incipient wetness method were almost inactive for the isopropanol dehydration due to the presence of an HPA fraction weakly attached to the support surface. Subsequent studies performed for the dehydration of several alcohols over TPA and molybdophosphoric acid supported on AC catalysts showed that the alcohol conversion depended on their molecular size.⁷¹ Moreover, selectivity to alkenes depended on the cyclodimer molecular size, whose formation decreased with a larger dimer size.

DuPont *et al.*⁷² showed that the acidic properties are retained in heteropolyacid supported ACs. They proved that HPA supported ACs are efficient catalysts for esterification reactions in the liquid phase.⁷³ They realized that the activity loss increases with the surface area of the carbon support and, for a particular support, it decreases with the polyanion



Scheme 18 Oxidation of cyclohexane to cyclohexanol and cyclohexanone over gold(III) C-scorpionate complexes supported on carbon materials.

loading.⁷⁴ In addition, the deactivation of the catalyst occurred during the recycling due to the leaching of the HPA from the support.

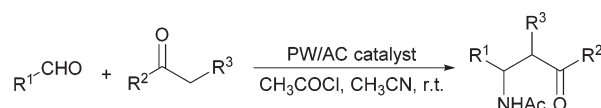
Tungstophosphoric acid (PW) supported on AC catalysts were used to synthesize β -acetamido ketones by the Dakin–West reaction (Scheme 19).⁷⁵ PW/C catalysts, prepared by the pore filling impregnation technique, showed high yields and better reusability *versus* the other supports used. Then, the PW/C catalysts were used under solvent-free conditions to synthesize 1,4-dihydropyridines from various aldehydes, β -dicarbonyl compounds and amines,⁷⁶ and in the condensation of aniline with ethyl acetoacetate to afford β -enaminones.⁷⁷ The PW/AC catalysts have also been used in the acetylation of glycerol.⁷⁸ In this last study, the catalytic activity increased with the amount of PW immobilized on the AC, except for high loading of PW, likely due to some hindrance in the porous system of the AC.

More recently, HPAs have been supported on AC fibers (ACF) as catalysts in the biodiesel synthesis.⁷⁹ The use of ACF as a catalytic support in liquid reactions is more suitable than conventional AC due to their particular features, such as smaller hydrodynamic resistance, fibrous shape, high mass transfer rates and easy removal from the reaction medium. On the other hand, Abdullah *et al.*⁸⁰ implemented an ultrasound-assisted biodiesel production process catalyzed by AC-supported tungstophosphoric acid catalysts.

2.5 Gold ACs

In the past two decades, gold catalysis has seen an exponential growth leading to the development of many synthetic transformations of considerable importance for the build-up of complex molecular systems, both under homo- and heterogeneous conditions. Supported gold-based catalysts have proven important for both environmental requirements and chemical industrial applications and, in particular, for fine chemical applications.⁸¹ Specifically, ACs are the most studied carbon-based material as supports and several research groups have demonstrated the activity of AC-supported Au catalysts in various chemical reactions. Therefore, due to their relevance and the growing number of publications in the past years, this field deserves a separated subsection.

One of the pioneers in the preparation of gold supported AC catalysts was García *et al.*⁸² This research group carried out the benzannulation reaction between 2-phenylethynylbenzaldehyde and phenylacetylene over gold nanoparticles supported on AC (Au/AC) catalysts. The Au/AC catalysts had high selectivity at full conversion under the same reaction conditions as the homogeneous catalysis with soluble AuCl₃. The catalyst could



Scheme 19 Synthesis of β -acetamido ketones over tungstophosphoric acid (PW) supported on activated carbon (AC).

be reused up to four times without loss of activity or selectivity with minor leaching of the inactive gold species.

The catalytic performance of gold supported on AC (Au/C) catalysts in hydrochlorination reactions has been widely investigated. Several strategies have been considered in order to improve the catalytic performance of the Au/C catalysts in this reaction. Thus, Wittanadecha and coworkers⁸³ prepared Au/C catalysts by different methods, such as ultrasonic-assisted, microwave-assisted, and conventional incipient wetness impregnation techniques, to test them in the hydrochlorination of acetylene. The better results were obtained in the case of the Au/C catalysts prepared by the ultrasonic-assisted technique (conversion > 80% and a selectivity to vinyl chloride monomer of 99.5% after 20 h). The effect of pre-treatment seemed to influence the catalytic activity of the Au/C catalysts. Thus, the presence of the Au³⁺ species on the catalyst surface led to the maximum initial catalyst activity.

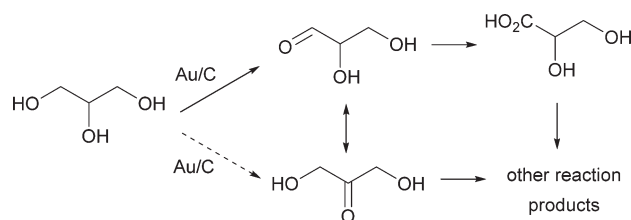
On the other hand, Wang *et al.*⁸⁴ studied the influence of different levels of oxygenated groups on the surface of Au/C catalysts having similar textural parameters in acetylene hydrochlorination. They concluded that phenol, ether, and carbonyl groups on the AC surface are responsible for the catalytic activity and stability of the Au/C catalysts. Huang *et al.*⁸⁵ carried out the acetylene hydrochlorination over TiO₂-AuCl₃/AC catalysts by the addition of TiO₂ species to the AuCl₃/AC catalysts. It seems that the TiO₂ species in the TiO₂-AuCl₃/AC catalysts relatively inhibited the reduction of Au³⁺ to Au⁰ and strengthened the adsorption of hydrogen chloride in acetylene hydrochlorination due to the strong interaction between the Au³⁺ active sites and the TiO₂ species. Reduction of the Au³⁺ species to metallic Au⁰ species was believed to be the predominant reason for the quick deactivation of the Au-based catalysts.

The support effect, as well as the introduction of a second metal, has been deeply investigated in order to increase the catalytic performance of gold-supported AC catalysts. Regarding that, Zhang *et al.*⁸⁶ studied the ternary Au-Co(III)-Cu(II) catalyst supported on spherical AC in the acetylene hydrochlorination. Its catalytic activity appeared to be due to the presence of the synergistic effects of Co(III) and Cu(II) that enhanced the adsorption of hydrogen chloride on the catalysts, increasing the amount of the active species Au⁺ and Au³⁺. The results obtained (99.7% acetylene conversion, 99.9% selectivity to vinyl chloride, and 6513 h of estimated lifetime) suggested the potential industrial applications of this catalyst. Bonarowska *et al.*⁸⁷ proved that AC-supported Pd-Au catalysts were more active catalysts in the hydrodechlorination of tetrachloromethane than the monometallic Pd catalysts due to the synergistic effects observed for the Pd-Au alloys. The Pd-Au intermixing was crucial to obtain the desired synergistic effect. The improved deactivation resistance associated with the reduced retention of the surface chlorine and carbonaceous species during hydrodechlorination was responsible for the higher total activity and better selectivity towards the hydrocarbon products.

Gold supported AC catalysts have also been used in the oxidation reactions of carbohydrates and alcohols, among others. Okatsu *et al.*⁸⁸ have reported for the first time that highly dispersed Au nanoparticles on AC exhibited a relatively high catalytic activity on the glucose oxidation reaction. They described that the Au nanoparticles could be deposited on AC directly from the gold precursor compounds by a deposition reduction method and, more effectively, by a solid grinding method. Hermans *et al.*⁸⁹ prepared Au/C and Au-Pd/C catalysts by an adsorption method, optimizing the process by managing the precursor-support interactions. The bimetallic catalysts were more active in glucose oxidation than their monometallic analogues, due to the synergistic effect between the Au and Pd metals. The metal incorporation order, the oxidation state and the activating agent used also influenced the catalytic performance.

Gold catalysts seem to be more resistant to oxygen poisoning and selective for the oxidation of primary alcohols, such as glycerol (Scheme 20). Demirel *et al.*⁹⁰ reported the oxidation of glycerol over gold supported on carbonaceous materials showing that the textural properties of the support can influence the product distribution. Thus, gold nanoparticles supported on CNTs displayed better activity and selectivity to dihydroxyacetone than the gold supported on activated carbon catalysts. Later, Rodrigues *et al.*⁹¹ performed the oxidation of glycerol over gold catalysts prepared by using a set of modified activated carbons with different levels of oxygenated functional groups on the surface, but with no significant differences in their textural parameters. Thus, gold particles with similar average sizes led to different performances: the presence of surface oxygenated acid groups inhibited the catalytic activity, whereas basic oxygen-free supports led to more active catalysts. However, the presence of oxygenated groups on the AC support does not influence significantly the selectivities. Other research groups have prepared gold supported on AC catalysts by the gold-sol method. The Au/AC catalysts prepared by sol immobilization displayed a better gold dispersion and a smaller gold particle size showing better catalytic activity in glycerol oxidation.⁹² On the other hand, Domínguez *et al.*⁹³ reported gold nanoparticles supported on AC (Au/AC) as catalysts in the catalytic wet peroxide oxidation of phenolic wastewater. The catalyst suffers rapid deactivation but its activity can be completely restored by an oxidative thermal treatment at 200 °C.

Nevertheless, it seems that combinations of gold with platinum group metals have exhibited potential for industrial applications, and in particular, Pd-Au catalysts supported on



Scheme 20 Glycerol oxidation over gold supported on carbonaceous materials.

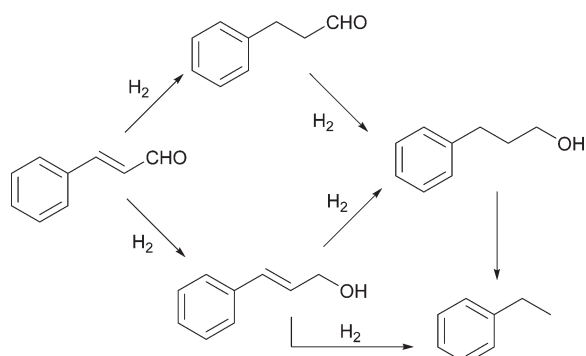
carbon for liquid phase oxidations and hydrogenations, as displayed below. It was shown that alloying Pd to Au nanoparticles led to a significant enhancement of the catalytic activity in the selective oxidation of glycerol, also increasing the durability of the catalyst.⁹⁴ Dimitratos *et al.*⁹⁵ carried out the liquid phase oxidation of glycerol over gold–palladium nanoparticles supported on AC. The control of selectivity could be possible when the appropriate reaction conditions were selected, while the activity was strongly dependent on the catalyst amount and the concentration of the base. Szumelda *et al.*⁹⁶ performed the hydrogenation of cinnamaldehyde in the liquid phase on AC PdAu catalysts (Scheme 21). Apparently, the Au content affected both the activity and selectivity of the activated carbon PdAu catalysts for cinnamaldehyde hydrogenation. The surface composition of these catalysts and the geometric and electronic modifications of the Pd sites due to the Pd–Au interactions seemed to influence the activity and selectivity of the reaction.

3. Miscellaneous

As anticipated, the application of different nanocarbon generations in catalysis is a hot topic. In the following sections, we have summarized the most relevant advances in this promising research field. We have focused on significant members of a group of carbon nanoallotropes with sp^2 carbon atoms arranged in a hexagonal network. This common structure means that they all have some common properties, although they also have significant differences due to their different sizes and shapes. The simplest and most basic representative of this group is graphene, whereas carbon nanofibers (CNFs) and carbon nanotubes (CNTs) consist of stacked and curved graphene sheets arranged in various ways.

3.1 Graphene

Graphene has recently attracted much more attention in the scientific community due to its exceptional properties. In comparison with the other carbon allotropes, this nanomaterial offers the greatest intrinsic carrier mobility at room temperature, with a perfect atomic lattice and excellent mechanical, thermal, electrical and optical properties. All of



Scheme 21 Hydrogenation of cinnamaldehyde over PdAu supported on carbonaceous material catalysts.

these characteristics together with its high specific surface area and the possibility to interact with organic molecules through π -stacking interactions make graphene as the current support key material in the development of superior heterogeneous catalytic systems.⁹⁷ However, stabilization and functionalization of graphene *via* modification of materials are necessary to avoid the known undesired aggregation (stacked graphitic structures), which in turn extend its applications. These materials have been successfully tested, mainly, in catalytic hydrogenation, oxidation, and coupling reactions.

The activity and selectivity of Au-based catalysts for a variety of important synthetic reactions are widely recognized. This fact combined with the unique properties of graphene has contributed to the development of new Au nanocomposites with improved catalytic behavior. In this respect, Xie *et al.*⁹⁸ reported the synthesis of Au-based graphene catalysts for the oxidation of alcohols to aldehydes/ketones. Au nanoparticles (2–4 nm) were deposited on nitrogen-doped graphene nanosheets (NG) *via* the direct simple reduction method. The nitrogen atom doped graphene nanosheets (NG) play an essential role in stabilizing the Au nanoparticles serving as the anchoring sites for the Au seeds. Based on the studies carried out by some authors, a plausible mechanism was proposed for gold formation on NG where tetrachloroaurate(III) ions, $AuCl_4^-$, are firstly adsorbed at the N doping sites, and then reduced to Au(0) nuclei by using $NaBH_4$. The remaining $AuCl_4^-$ could be adsorbed endlessly on the surface of the as-formed gold nuclei and reduced to Au(0), leading to the growth of a gold nucleus, or adsorbed on a new reactive site and directly reduced to Au(0), forming a new nucleus (Fig. 3). In general, the average size of the gold supported nanoparticles did not vary with increasing gold loading. The catalytic behavior of this composite was evaluated in the aerobic selective oxidation of benzylic alcohols, at 343 K under aerobic conditions, in the presence of H_2O . The initial reaction of benzyl oxidation catalyzed by the Au/NG composites was notably higher than that over the Au/graphene catalysts.

Porous graphene oxide (p-GO) as a metal-free catalyst was recently reported by Su *et al.*⁹⁹ for the oxidative coupling of primary amines under aerobic conditions in tandem to produce a series of valuable products such as α -aminophosphonates, α -aminonitriles, and polycyclic heterocompounds. The authors described for the first time a bifunctional catalyst, Pd@p-GO, in which p-GO was decorated with Pd nanoparticles, able to simultaneously activate molecular oxygen and hydrogen for the tandem oxidation and hydrogenation reactions in the *N*-alkylation of primary amines, under mild conditions (Scheme 22).

The tentative mechanism for the tandem catalysis by Pd@p-GO consisted of i) the oxidative coupling reaction of the primary amine on the active defect sites producing the imine intermediates, and ii) the activation of the molecular hydrogen, in the presence of the Pd nanocatalyst, and the transfer to the imine intermediates leading to the secondary amine products (Fig. 4) with good to excellent yields.

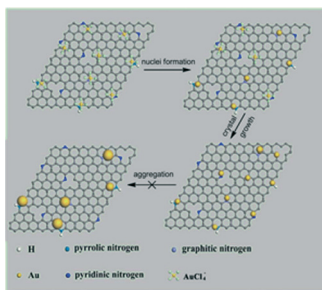
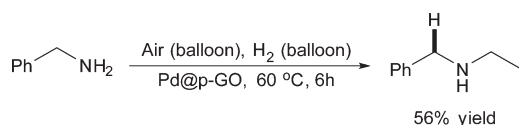


Fig. 3 Proposed mechanism of gold formation on nitrogen doped graphene. Reprinted with permission from ref. 98. Copyright © 2012 RSC.

Verma *et al.*¹⁰⁰ reported a magnetically separable GO-based catalyst, containing a uniform distribution of iron nanoparticles, for the oxidative cyanation of tertiary amines. Characterization of the composite by using the XRD and XPS techniques clearly indicated that the support was enriched with the crystalline Fe/FeO phases without any evidence of the presence of the Fe₂O₃ phase; the layer of FeO was present on the surface of the Fe(0) nanoparticles. The catalyst was tested in the oxidative cyanation of a variety of tertiary amines, in the presence of H₂O₂ and sodium cyanide, in acetic acid, yielding the corresponding α -aminonitriles with good to excellent yields (up to 77%) (Scheme 23). The active species for the reaction were the Fe(II) species and not the metallic iron.

As mentioned above, the most frequently used synthetic approach for the homogeneous catalyst immobilization consists of the covalent bond formation between the solid support and the ligand, implying the necessary functionalization of both species and originating changes in chemical reactivity. To this end, more recently Blanco *et al.*¹⁰¹ reported new, stable and reusable hybrid graphene-based-Ir-NHC materials (where NHC is N-heterocyclic carbene) (Fig. 5) for the hydrogen-transfer reduction of cyclohexanone to cyclohexanol.

These nanohybrids were prepared by the covalent functionalization of graphene oxide (GO) or thermally reduced graphene oxide (TRGO) as follows i) a reaction with *p*-nitrophenylchloroformate, through their OH⁻ surface groups, ii) subsequent covalent anchoring of a hydroxy-functionalized imidazolium salt and, finally, iii) by a subsequent reaction with [Ir(I-OMe)(cod)]₂. These catalysts were active in the heterogeneous hydrogen-transfer reduction of cyclohexanone to cyclohexanol using 2-propanol/KOH as the hydrogen source (Scheme 24). The TRGO-NHC-iridium



Scheme 22 Simultaneous activation of molecular oxygen and hydrogen.

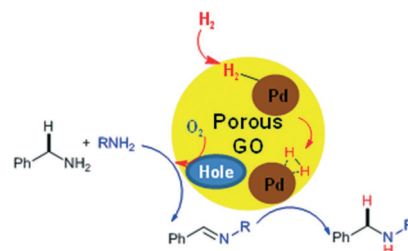
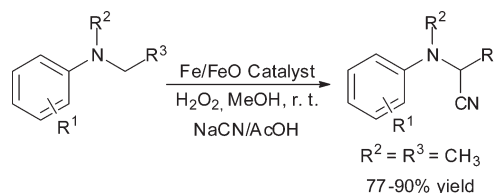


Fig. 4 Proposed mechanism for the Pd@p-GO bifunctional catalytic system.

hybrid catalyst showed not only the best catalytic performance (90% conversion after 150 min of reaction time) but also its activity, being slightly superior to that of the related acetoxy-functionalized NHC iridium homogeneous ones. The presence of remaining oxygen functional groups on the hybrid catalyst based on GO, as competitive sites, could be responsible for the lower catalytic performance observed.

The non-covalent interactions between graphene and polyaromatic hydrocarbons such as pyrene-derivatives emerge as an interesting, useful and alternative synthetic approach for the preparation of heterogeneous graphene-based catalysts. This synthetic route allows the introduction of the appropriate functional groups over the nanocarbon without affecting its electronic network. In this context, Sabater *et al.*¹⁰² described new nanostructured graphitic materials based on Pd and Ru complexes, prepared from an imidazolium salt substituted with pyrene moieties, which were immobilized onto the graphene oxide (rGO) surface by π -stacking interactions (Scheme 25). The catalytic behavior of these nanostructured hybrid materials was investigated in the ruthenium-catalyzed oxidation of alcohols and in the palladium-mediated hydrogenation of alkenes and nitroarenes (Schemes 26–28) giving rise to higher activities than the related homogeneous catalysts. The catalysts therein reported were recycled 10 times without loss of activity.

Cross-coupling reactions, such as the Heck, Suzuki and Sonogashira reactions, were also investigated in the presence of metal nanoparticles supported over GO. Concerning that, Moussa *et al.*¹⁰³ developed a new family of highly active Pd nanoparticle catalysts supported on partially reduced graphene oxide nanosheets for these types of transformations. Pd nanoparticles of different sizes were supported on partially reduced graphene nanosheets (Pd/PRGO) by pulsed laser irradiation of aqueous solutions of GO and palladium ions



Scheme 23 Oxidative cyanation of tertiary amines catalyzed by an iron-graphene nanocomposite.

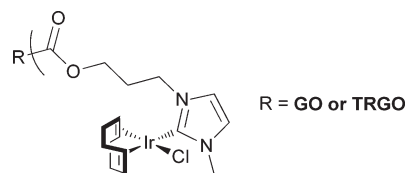
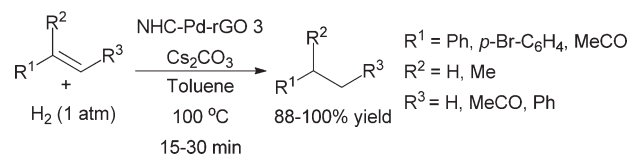
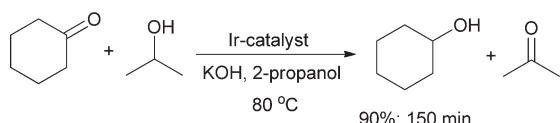


Fig. 5 Hybrid graphene-based Ir-NHC materials.



Scheme 26 Alkene hydrogenation using molecular hydrogen.



Scheme 24 Hydrogen transfer reduction of cyclohexanone to cyclohexanol.

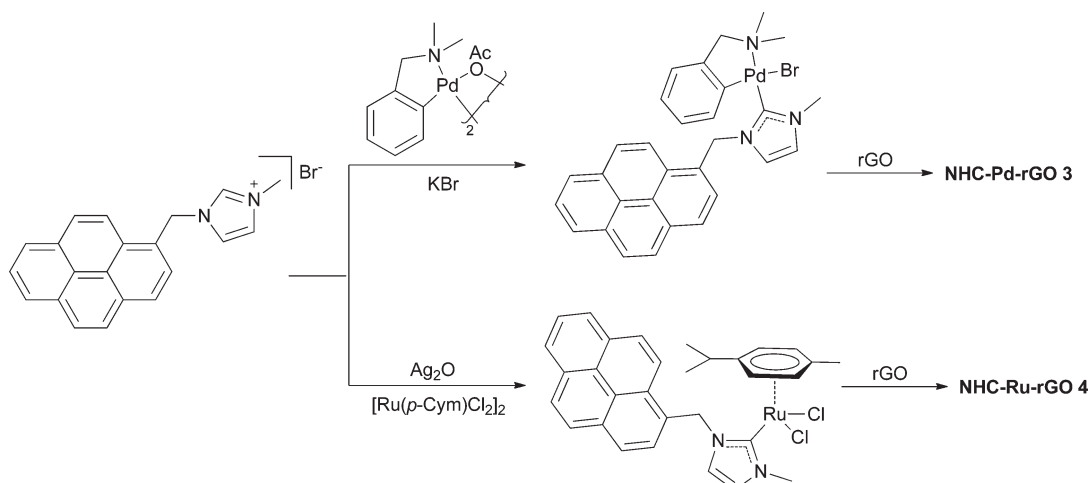
without the use of chemical reducing or capping agents. This process provoked the formation of multiple defects on the surface of the PRGO, providing an excellent environment for anchoring the Pd nanoparticles. These metal nanocarbons were active for the Suzuki cross coupling reactions affording biphenyl with an excellent yield (ranging from 80 to 95% after 8 h of reaction time), at room temperature, even when the catalyst loading was decreased to 0.008 mol%. The reaction was surprisingly fast working at 120 °C under MW irradiation (quantitative yield in only 5 min). The catalysts under study were also active in the Heck and Sonogashira cross coupling reactions, under MW irradiation, leading to the corresponding biaryls with excellent yields (Scheme 29).

In the same line, Santra *et al.*¹⁰⁴ reported the anchoring of Pd nanoparticles onto the GO sheet by pyrolysis, without using any external reducing agent, as a recyclable catalyst for the synthesis of biaryl cores for the Suzuki–Miyaura coupling reaction. The scope of the methodology was explored by synthesizing biaryls with a wide variety of functional group

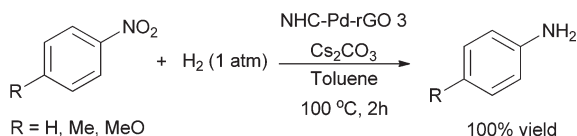
tolerance. Furthermore, this nanocarbon was a very efficient catalyst for the quantitative synthesis of the core constituents of top selling drugs, such as boscalid, telmisartan, and biologically active GSK376501A (Fig. 6).

Shaabani *et al.*¹⁰⁵ reported a highly active and reusable catalyst based on PdCo bimetallic nanoparticles supported on polypropylenimine (PPI)-grafted graphene for the carbon–carbon cross-coupling Sonogashira reactions, under solvent-free conditions, at room temperature, and ultrasound irradiation. The PPI dendrimer was synthesized by using a divergent strategy from malononitrile functionalized graphene as follows: i) reduction of CN to amine groups, ii) Michael addition of the amine groups to acrylonitrile and iii) subsequent reduction of the introduced CN groups. Finally, PdCo alloy nanoparticles were then attached *via* a co-complexation method. The catalytic activity of the bimetallic catalyst was notably higher than that observed for the individual nanoparticle (Pd or Co) catalysts (Scheme 30).

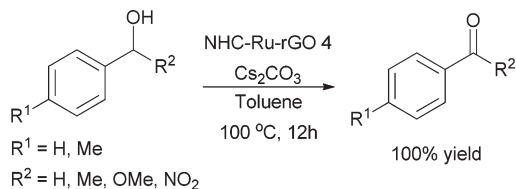
A similar strategy for the *in situ* growth of palladium and the assembly of Fe₃O₄ nanoparticles on reduced graphene oxide (rGO) dendrimers has been reported by Liu *et al.*¹⁰⁶ Pd/Fe₃O₄/PEI/rGO (where PEI is polyethyleneimine) is a highly active and reusable catalyst in the Tsuji–Trost reaction (Scheme 31). Pd/Fe₃O₄/PEI/rGO is easily removed from the reaction crude mixture with the simple application of an external magnetic field, and exhibiting the best catalytic performance when compared with the corresponding monometallic catalysts.



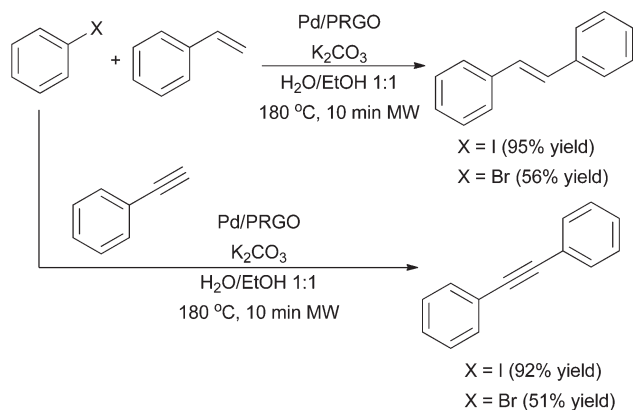
Scheme 25 Immobilization of Pd and Ru complexes, prepared from an imidazolium salt substituted with pyrene moieties, onto the graphene oxide (rGO) surface.



Scheme 27 Nitro reduction using molecular hydrogen.



Scheme 28 Oxidant free dehydrogenation of alcohols.



Scheme 29 Heck and Sonogashira coupling reactions catalyzed by Pd/PRGO.

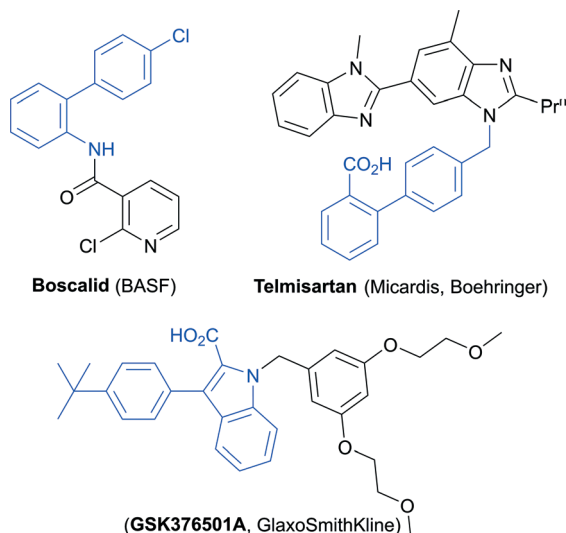


Fig. 6 Core constituents (in blue) of top selling drugs: boscalid, telmisartan, and GSK376501A.

Recently, the catalytic activity as a function of metal nanoparticle orientation on graphene substrates has been highlighted. Thus, oriented (1 1 1) copper nanoplatelets on

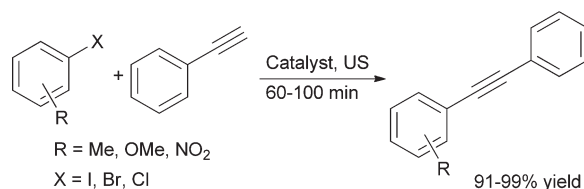
graphene undergo spontaneous oxidation to render oriented (2 0 0) Cu₂O nanoplatelets on few-layered graphene. These films containing oriented Cu₂O exhibit catalyst turnover numbers that can be three orders of magnitude higher for the Ullmann-type coupling, dehydrogenative coupling of dimethylphenylsilane with *n*-butanol and C–N cross-coupling than those of the analogous unoriented graphene-supported copper(i) oxide nanoplatelets.¹⁰⁷

Although the use of graphene has this successful progress, some key issues still need to be addressed on the way forward. Thus, the preparation of perfect graphene sheets lags far behind the great demands on their practical applications. The recent exfoliation method¹⁰⁸ can hardly provide a uniform and clean single layer of graphene, while the commonly used oxidation–reduction pathway is bothered with the introduction of defects and decrease in the transport properties. As a consequence, the lack of an effective way to ideal graphene has gradually become one of the biggest bottlenecks for making further improvement in the performance of the assembled structures.

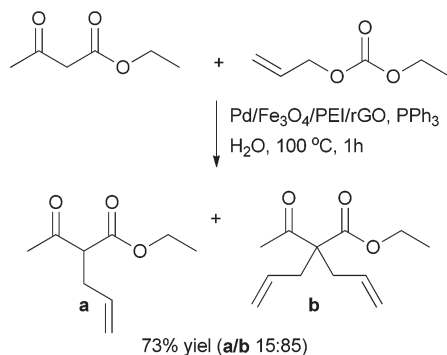
3.2 Nanofibers

Carbon nanofibers (CNFs) are a noncontinuous 1D carbon nanoallotrope of cylindrical or conical shape, consisting of stacked and curved graphene sheets arranged in various ways.¹⁰⁹ They were identified and extensively studied long back before the discovery CNTs. They are frequently described as sp²-based linear filaments with a diameter ranging from 50 to 200 nm and a high aspect ratio exceeding 100. Depending on the internal structure of the CNF (*i.e.*, the way the graphene sheets are arranged), the types of CNF are i) platelet-type (p-CNF), ii) ribbon or tubular-type (t-CNF), and iii) fishbone-type CNF (f-CNF)¹¹⁰ with the graphite layers perpendicular, parallel, and tilted to the principal axis, respectively (Fig. 7).

Moreover, three topological structures have been proposed to represent the f-CNF morphology: i) the stacked-up and ii) cone-stacked CNFs, with a similar structure composed of truncated cones arranged to leave a hollow core, and iii) cone-helix CNFs with a graphite layer forming a continuous helix–spiral architecture and with an internal hollow core. The orientation of the graphite layers, and hence the basal-to-edge surface area ratio, has been found to have significant effects on the catalytic activity and selectivity of CNFs.¹¹¹ α is defined as the position of the graphene sheet near the



Scheme 30 Sonogashira cross coupling catalyzed by PdCo bimetallic nanoparticles supported on polypropylenimine (PPI)-grafted graphene.



Scheme 31 Tsuji-Trost reaction catalyzed by Pd/Fe₃O₄/PEI/rGO.

sidewall surface with respect to the axis of the CNF and this angle determines the physicochemical properties of the CNFs. Thus, CNFs with cone and tilted-graphene sheet motifs are characterized with $\alpha > 0$.

CNFs have unique features and specific characteristics, such as fibrous structures, high resistance to strong acids and bases, porosity, high electric conductivity (similar to graphite), high surface area (80–200 m² g⁻¹), well-defined nanostructures, easily tuned mesoporous properties, and high mechanical strength.¹¹² These interesting properties of these 1D-structured carbon nanomaterials have been intensively reviewed¹¹³ and exploited in many applications, such as catalysts and catalyst support materials,^{109,114} functional components of electronic devices (biosensors, anodes in lithium ion batteries, electrodes in fuel cells),¹¹⁵ materials for gas storage,¹¹⁶ and polymer additives in the formation of composites to improve their chemical, thermal, and electrical features.¹¹⁷ Herein, we focus on their use in the catalysis field.

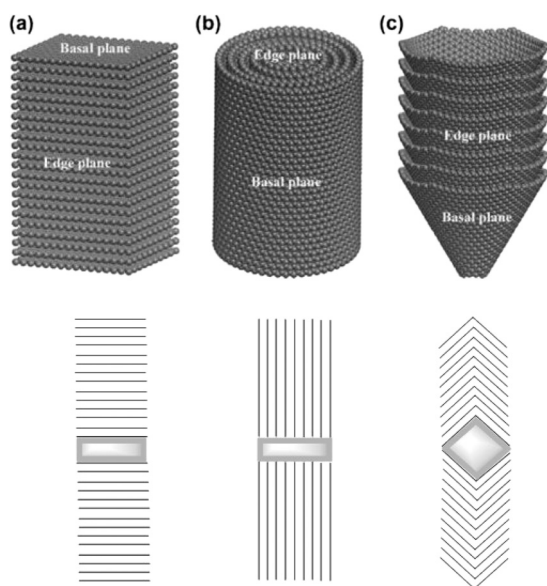


Fig. 7 Schematic representations of CNFs with different basal-to-edge surface area ratios: (a) platelet-type CNF, (b) ribbon/tubular-type CNF, and (c) fishbone-type CNF. Adapted from ref. 111 with permission from Elsevier. Copyright © 2012.

The use of CNFs as catalyst supports and/or directly as catalysts has been an active topic of research¹¹⁸ since the first report published in 1994.¹¹⁴ Their properties can exert a significant impact compared to the traditional carbon or oxide supports. The following characteristics make CNFs attractive as catalysts and catalyst supports: i) the presence of a large number of edges in CNFs provides anchoring sites for catalyst precursors. Modern techniques have made it possible to control the surface geometric structure and surface chemistry of CNFs,¹¹⁹ which opens up opportunities to tailor the properties of both the CNF surface and its supported metal nanoparticles; ii) the surface properties of CNFs (and CNTs) can be easily adjusted by surface oxidation, foreign-ion doping (*i.e.*, nitrogen or boron), or by using the confinement effect so as to fulfill the different requirements for different applications; iii) as catalyst supports, CNFs offer some unique advantages over the more traditional materials, such as alumina or silica, because CNFs (and CNTs) exhibit high surface area and are also heat and electrical crystallite conductors, so strong interactions can be formed between the metal atoms and the CNTs/CNFs. As a consequence, modification of the morphological characteristics of the catalyst particles could give rise to unexpected activity and selectivity patterns. The combination of structural and electrical properties makes CNTs/CNFs very attractive as candidates for exploitation both as catalysts and catalyst supports; iv) CNTs and CNFs mostly consist of mesopores with large external surfaces, which make them superior supports for fast reactions in the gas and liquid phases and for complex reactions in which the products are not chemically stable. Compared to traditional carbon materials, in particular to AC, mass-transfer limitations during the reaction can be reduced so that the activity and selectivity would be enhanced.

Their graphitic structure leads to metal-support interactions and an electron transfer between the metal particles and the graphitic support (electronic perturbation) which can improve the catalytic activity/selectivity. The CNF structure has a remarkable influence on the interactions, due to the different edge-site-to-basal-plane ratios, and the edge sites and defects form much stronger bonds with the metals, thus leading to strong interactions. The interactions of metals with CNFs follow the order: platelets > fishbones > tubes. Metal/CNF surface interactions influence the dispersion, stability, as well as the redox potential of the metal, which can be tailored to improve the activity for catalytic reactions that involve redox cycles.^{112,120}

The effective utilization of the high-surface-area mesoporous structure of 1D carbon nanomaterials (CNTs and CNFs) in catalysis through improved dispersion of the metal or metal-oxide nanoparticles has been widely explored in the literature¹²¹ and some key examples are shown in Table 2. High selectivities have been observed in these catalytic systems displaying different metal-support interactions and/or charge transfer phenomena compared to those on other supports, such as ACs or alumina.

3.3 Carbon Nanotubes

CNTs and CNFs show notably different nanostructures and properties, despite both containing curved sp^2 -hybridized carbon atoms. The main difference involves the configuration of the underlying planes that are created by the alignment of the carbon atoms. CNTs display an axial alignment of the concentric cylindrical planes that are mainly composed of hexagonal substructures. In this sense, CNTs can be sub-classified into single-walled carbon nanotubes (SWCNTs, diameters of around 0.4–2 nm and are several micrometers long, with an empty internal space), and multi-walled carbon nanotubes (MWCNTs) by considering the number of axially aligned cylindrical tubes. The aspect ratio (*i.e.*, length-to-diameter ratio) of carbon nanotubes frequently exceeds 10 000, and thus, they are regarded as the most anisotropic materials ever produced. Apart from the diameter and the length, chirality (the angle between the hexagons and the nanotube axis) is another key parameter of the carbon nanotubes. Depending on the chirality, the carbon atoms around the nanotube circumference can be arranged in several ways: the armchair, zigzag, and chiral patterns are the

most common examples.¹⁴⁴ As a result of the differences between the ratios of the edge planes to the basal planes, CNTs are thus differentiated from CNFs in key electronic properties and surface (re)activity behavior.¹⁴⁵

Since the discovery of multi-wall carbon nanotubes (MWNT) by Iijima,¹⁴⁶ CNTs have become one of the most active fields of nanoscience and nanotechnology due to their exceptional properties that make them suitable for many potential applications as polymer reinforcements for composites or breakthrough materials for energy storage, electronics and catalysis.

Due to the high strength of the covalent C=C bonds between adjacent sp^2 carbon atoms, CNTs are the strongest yet known materials with a high flexibility. SWNTs have shown remarkable superplasticity, becoming nearly 280% longer and 15 times narrower before breaking, which is explained in terms of the nucleation and motion of kinks in the structure.^{147,148}

The electronic properties of SWNTs are mainly governed by two factors: the tube diameter and the helicity, which is defined by the way in which the graphene layer is rolled up¹⁴⁹ (armchair, zigzag or chiral). In particular, armchair

Table 2 Representative examples of metal–CNF catalysts

Catalyst	Reaction	Ref.	Results
	<i>Hydrogenation</i>		
Ni/CNF	Alkene hydrogenations	122	Reaction sensitive to the nature of the metal–support interaction
Rh/CNF	Cyclohexene	123	Activity independent of the nanoparticle size. Influence of oxygen-containing species present on the surfaces of the support
Ru/CNF	Arene	124	Excellent catalytic activity
Pd/CNF	Phenol	125	Complete hydrogenation to alcohol
Ni/CNF	Crotonaldehyde	126	Formation of crotyl alcohol with higher selectivity than with γ -Al ₂ O ₃
Pd/CNF	Cinnamaldehyde	127	Selective hydrogenation of C=C. More active than Pd/AC
Ru/CNF	Cinnamaldehyde	128	Crucial role of cinnamaldehyde adsorption on the support
	<i>Dehydrogenation</i>		
Pt/CNF	Hydrogen production from decaline	129	Performance strongly affected by the metal particle dispersion
	<i>Involving CO/H₂ reactions</i>		
Co–Cu/CNF	Alcohol synthesis	130	Selectivity towards the formation of higher alcohols (butanol)
Rh/CNF	Hydroformylation of ethylene	131	Higher selectivity than Rh/SiO ₂ , probably due to the hexagonal shape of the rhodium crystallites
Ru/CNF and Ru–Ba/CNF	<i>Ammonia synthesis</i>	132	More active than AC due to the high purity of the support
	<i>Biomass conversion</i>		
Ru/CNF	Hydrogenolysis of sorbitol to glycols	133	Better behavior than Ru/AC due to the higher Ru dispersion on CNF
Ni/CNF	Hydrolytic hydrogenation of cellulose to C6 sugar alcohols	134	Appropriate catalyst balance between Ni dispersion and hydrogenation capacity, and the number of acidic surface-oxygen groups responsible for the acid-catalyzed hydrolysis
	<i>Oxidation reactions</i>		
Pt/S–CNFs	Glycerol with molecular oxygen	135	Selective formation of glycerin acid in a base-free aqueous solution
Cu/CNF, Ni/CNF	Ethylene glycol and glycerol to organic acids	136	Under anaerobic aqueous conditions
RuO ₂ /CNF	Alcohols to aldehydes	137	Superiority over Ru–ACs under aerobic conditions; high metal dispersion
	<i>Other reactions</i>		
Pt/CNF	Skeletal <i>n</i> -hexane reaction	138	Better activity and isomer formation on Pt/f-CNF than on Pt/p-CNF
La ₂ O ₃ /CNF	Self-condensation reaction of acetone to diacetone	139	Superior catalytic activity to the optimized bulk La ₂ O ₃
LaCl ₃ /CNF	Dechlorination of hydrocarbons	140	
Pd/CNF	Heck reaction	141	The activity increased exponentially with a decrease in the Pd particle size, low sensitivity towards oxygen, and high stability in multi-cycles
Ir/f-CNF	Hydrazine decomposition	142	Better performance than a commercial Ir/Al ₂ O ₃ catalyst
Hydrotalcites/CNF	M1BK synthesis	143	Specific activity four times higher than that of the unsupported catalyst

SWNTs are metallic and the zigzag ones display a semiconductor behavior. The rolling up of the graphene layers can vary along the different walls of a single MWNT, so a fine prediction of the electronic properties is more difficult.

CNTs present specific adsorption properties when compared to graphite or to AC, mainly due to their peculiar morphology, the role of defects, opening/closing of the tubes, chemical purification or the presence of impurities as catalyst particles. Other important factors in the final activity and reproducibility of the catalytic system are the resistance to abrasion and dimensional and thermal stabilities. In particular, and analogously to CNFs, they could replace ACs in liquid-phase reactions since the properties of ACs are still difficult to control and their microporosity has often slowed down catalyst development.

CNTs are not dispersible in organic solvents or water and are usually held strongly together in bundles by significant van der Waals interactions.^{150,151} A similar group of cylindrical carbon nanostructures that have recently appeared in the literature are referred to as bamboo-like CNTs due to the division of their internal spaces into small cavities similar to those found in bamboo.¹⁵²

The syntheses of CNTs have been intensively reviewed,¹⁵³ although a general principle for the rational design of carbon nanomaterials in a controlled manner is yet to be established.

In contrast to porous carbons, the large surface areas of the external surfaces of CNTs are ideal for the immobilization of metallic or metal oxide nanoparticles that are used in catalytic systems, since they allow better contact between the reactant and the catalytic component. Electronic effects that are derived from interactions between the metal and the support can endow the catalyst particles with unusual properties. The deposition of metal nanoparticles on CNTs has been reviewed extensively by several groups.¹⁵⁴

First-principles electronic-structure calculations indicate that the energy barrier of metal-atom diffusion is much lower on the CNT sidewall than on the CNF edge.¹⁵⁵ Thus, metal-catalyst agglomeration occurs very readily on the CNT surface and causes low metal dispersion. These different features in CNTs and CNFs have consequences on their catalytic properties if they are used as catalyst supports.¹¹³

In parallel to the growing knowledge on the synthesis and understanding of nanocarbon materials, their use as advanced catalysts moved to more rational bases. As noted above for CNFs, the engineering of CNTs makes it possible to control the arrangement of the carbon atoms, providing opportunities to tailor the properties of both the CNT surface and its supported metal nanoparticles. Table 3 shows their relevant applications as supports in synthesis.

To improve the catalytic activity of CNTs, heteroatom-containing functional groups can be introduced onto the surface of CNTs. Thus, nitrogen, oxygen, phosphorous, sulphur and boron can be used to modify the surface chemistry of CNTs.¹⁵⁶ In addition, the lack of solubility and the difficult manipulation of CNTs in most solvents have limited their

use. Therefore, CNTs generally need to undergo chemical functionalization to enhance their solubility in various solvents and to produce novel hybrid materials for practical applications.¹⁵⁷

Doping of CNTs with nitrogen improves the physical properties of CNTs by introducing surface defects into the graphene structure of N-CNTs. Such surface defects promote N-CNT surface wetting resulting in increased catalytic activity.¹⁵⁸ However, it should be noted that the available types of catalyst preparation depend on the surface properties. For instance, Pt particles are uniformly dispersed over these materials and they have a smaller average particle size than on non-nitrogen-doped carbon supports. This dispersion helps to increase the catalytic activity of the metal in various reactions, such as oxygen-reduction reactions,¹⁵⁹ both hydrogen-oxidation and oxygen-reduction reactions in proton-exchange membrane fuel cells¹⁶⁰ or the hydrogenation of nitroarenes.¹⁶¹

The edge structure, with various edge-site-to-basal-plane ratios, and the functional groups on the edge sites have a significant influence on the electron localization and, thus, the proton affinity of these materials. Oxygen-free or N-doped edge sites have a strong basicity, which contribute to better anchoring of the metal nanoparticles and improve the catalytic performance of these carbon materials.¹⁶² Accordingly, the improved chemical and electrical properties of N-doped CNTs have been observed which result in the activation of the metal catalyst¹⁶³ and enhancement of the binding energy between the N-CNTs and the metal catalysts.¹⁶⁴ For instance, Nyamori *et al.*¹⁶⁵ have recently reported that pyrrolic Pd/N-CNTs exhibited high yields and a higher selectivity towards aminobenzophenone in the hydrogenation of nitrobenzophenone than Pd on carbon nanotubes and Pd on AC (Scheme 32). The enhanced selectivity towards nitroreduction over *p*-benzylamine observed with Pd/N-CNTs was attributed to the promoting effect of pyrrolic-N.

There is a large potential for the development and application of an organic polymer with tailored physical and chemical properties in both selective catalysis and functional materials science.¹⁶⁶ Therefore, to combine the advantages of polymers (nitrogen-containing polymers) and CNTs, much effort has been put in polymer/CNT composite materials. Thus, for instance, the composite material poly(4-vinylpyridine)-functionalized carbon nanotubes (PVP/CNT), through the formation of the coordinative bond $N:\rightarrow Ru^{3+}$, shows interesting properties. The ruthenium complex immobilized on PVP/CNT (Ru-PVP/CNT) catalyst reveals excellent catalytic performance towards selective aerobic oxidation of biomass-based 5-hydroxymethylfurfural to 2,5-diformylfuran¹⁶⁷ (Fig. 8).

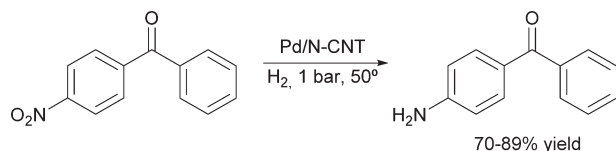
It has been recently realized that metal nanoparticles can be effectively stabilized against coalescence by encapsulation within metal oxide layers, such as SiO₂ shells. The catalytic results showed that Pt@CNT/SiO₂ was active for the hydrogenation of nitrobenzene with a very high activity comparable to that of Pt@CNT.¹⁶⁸

Table 3 Representative examples of metal–CNT catalysts

Catalyst	Reaction	Reference	Results
	<i>Hydrogenation</i>		
Pd/MWNT	1-Octyne	169	High stability
Pt/CNT	Nitrobenzene	170	Excellent activity highly because of the dispersed Pt and the mesoporous structure of the acid-oxidized CNT-supported Pt catalyst
Pt@CNT/SiO ₂	Nitrobenzene	168	Very high activity comparable to that of Pt@CNT
Pd/N-CNTs	Nitrobenzophenone	165	Higher selectivity to aminobenzophenone than Pd on CNTs and Pd on AC due to the promoting effect of pyrrolic-N
Pt/SWNT	Prenal (3-methyl-2-butenal) to prenil (3-methyl-2-butenol)	171	Active and selective
Co–Pt/SWNT	Cinnamaldehyde	172	High activity and selective hydrogenation to cinnamyl alcohol due to the mesoporous structure
Ru–Pt/MWNT	Cinnamaldehyde	173	Mesoporous nanostructured support makes mass-transfer limitations less significant and gives much higher activities. Higher selectivity than that obtained with the monometallic systems.
Rh/MWNT	Cinnamaldehyde	174	High selectivity and catalytic activity three times higher than the corresponding Rh/C* catalyst
	<i>Dehydrogenation</i>		
Co/MWNT	Cyclohexanol to cyclohexanone	175	Activity and selectivity towards cyclohexanone slightly higher than on Co/C*
CeO ₂ /CNT	Ethylbenzene to styrene	176	Showed an important confinement effect. Shorter CNTs filled with CeO ₂ exhibit higher catalytic activities due to the decreasing diffusion resistance of the reactants and products in the CNT channels
Rh/MWNT	Hydroformylation of hex-1-ene	174b	More active than a Rh/C* catalyst
[HRh(CO)(PPh ₃) ₃]/MWNT	Hydroformylation of propylene	177	Higher conversion and regioselectivity towards <i>n</i> -butyraldehyde than on similar systems on AC, carbon molecular sieves and silica
	<i>CO/H₂ reactions</i>		
Ru/MWNT	Ammonia synthesis	178	Potassium promoted ruthenium catalysts supported on MWNT were much more active than their counterparts deposited on graphite or fullerenes, due to the higher surface area of the nanotubes that allows a better dispersion of the metallic phase and to the electronic properties of this support that could enhance the electron transfer from potassium to ruthenium
	<i>Biomass conversion</i>		
Ru/CNT	Cellulose to C2–C6 polyols	179	The CNTs promote the hydrolysis of cellulose into a reduced sugar
Ru–PVP/CNT	Oxidation of 5-hydroxymethylfurfural to 2,5-diformylfuran	167	Excellent catalytic performance and selectivity
Ni/MWNT	Pyrolysis of bio-oil	180	The uniform and narrow distribution of small Ni particles on the CNTs lead to excellent low-temperature reforming of oxygenated organic compounds in bio-oil
Au/MWNT	Oxidation of glycerol	181	High selectivity for the oxidation of the secondary hydroxyl group to form dihydroxyacetone, independent of the preparation method
Mo ₂ C/CNT	Hydrogenation of levulinic acid to γ -valerolactone	182	When the carbide nanoparticles are positioned within the carbon nanotubes, conversions and selectivities are above 90%
	<i>Oxidation reactions</i>		
Pt/MWNT	MeOH oxidation	183	Better performance than Pt-on-carbon-black, due to its large external surface area and crystalline structure
Pd/MnO _x /CNT	Alcohol oxidations	184	The catalytic activity correlated with MnO _x loading, indicating the important role of manganese oxide in tuning the properties of the Pd catalytically active sites
W/MWNT	Epoxidation of alkenes	185	W(CO) ₆ supported on MWCNTs modified with 1,2-diaminobenzene is an efficient catalyst for a wide range of linear and cyclic alkenes
Pt/CNT, Cu/CNT, Ru/CNT	Aniline oxidation	186	High external surface area and the absence of micropores provide an efficient surface contact between an aniline molecule and the active sites
	<i>Other reactions</i>		
Co/MWNT under sonication	Synthesis of mono- and disubstituted dihydroquinazolines through three-component condensation	187	Excellent catalytic performance
Pd/CNT	Cross-coupling, Suzuki–Miyaura	188	Pd nanoparticles deposited on MWNT possess the most functional catalytic properties, with optimum activity, stability and recyclability in a range of cross-coupling reactions
Pd/MWNT	Hydrodehalogenation of aryl halides	189	The CNTs could significantly influence the catalytic activities of the CNT-supported metal catalysts

On other hand, it is known that the well-defined channels of CNTs can be used to introduce metallic and metal oxide nanoparticles into the CNT cavity and investigate their effects

on the catalytic performance. Recent results have shown that encapsulated nanoparticles inside CNT channels have better catalytic performance compared to those on conventional



Scheme 32 Hydrogenation of nitrobenzophenone over pyrrolic Pd/N-CNTs.

catalysts.^{118b,190} The confinement of nanoparticles inside the CNTs and their catalytic applications have been recently reviewed by Pan and Bao.¹⁹¹ For instance, combined DFT investigations, CO adsorption, and ammonia synthesis have consistently indicated that the electron density of Ru particles outside the CNTs is higher than those confined inside the CNTs.¹⁹² This difference is ascribed to the curvature of the graphene sheet and to the higher energy density of graphene on the outside than on the inside of the CNTs. Ammonia synthesis¹⁹³ and decomposition¹⁹⁴ have been used as probe reactions to investigate the electronic properties of Ru nanoparticles on and inside the CNTs, because the adsorption and recombination of N atoms are normally very sensitive to the electronic properties of the metallic nanoparticles. The turnover frequencies (TOFs) of ammonia synthesis over Ru-out were much higher than on Ru-in.

It has also been recognized that the electron densities of the graphene sheets inside and outside the CNTs influence the interactions of metal oxides with CNTs. It is much easier to reduce the metal oxides inside the CNTs than on the outside, due to different interactions.^{190,191}

Additionally, improved selectivity towards the desired product when metal/CNT catalysts are used can also be attributed to nano-confinement of the substrate molecule infused into the CNTs.¹⁹⁵ The confinement mainly modifies the electronic properties of the active phase, promotes the redox properties of metal oxides and improves the states of gas-phase reactants inside CNTs during catalytic reactions. Nevertheless, due to synthetic difficulty, the confinement effect of CNT channels for these materials is limitedly applied in the catalytic reactions.

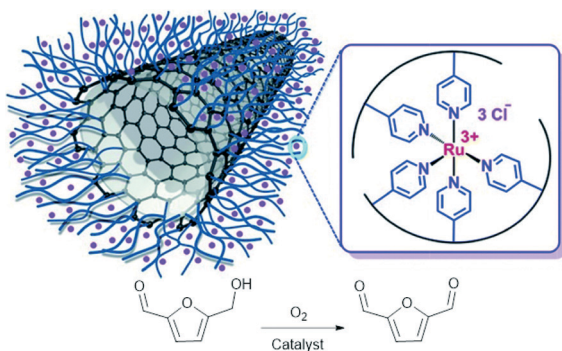


Fig. 8 Proposed structure of a Ru-PVP/CNT for the selective oxidation of 5-hydroxymethylfurfural with permission from ref. 167. Copyright © 2015 RSC.

Of growing interest also is the area of the designing nano-carbon–nanocarbon hybrids and hierarchical systems generated by combining different carbon nanostructures, such as functionalized fullerenes linked to CNTs (nanobuds), in order to develop multifunctional superstructures.^{195–198} In this sense, CNT-based aerogels,¹⁹⁹ a novel approach to develop CNT networks, are promising for catalysis, serving as either scaffolds or as the catalysts themselves. The rational use of CNT-based aerogels as supports to load catalytic matter can create high-performance catalysts.²⁰⁰

Unlike traditional catalysts where the reaction only occurs at the external surface, the aerogel-supported metal catalyst allows a “bulk phase” catalysis throughout the gel network because of its porous structure.²⁰¹ In summary, the combination of carbon nanostructures and different nanoscopic species within a composite material is expected to result in the enhancement of their functional properties and can lead to new synergistic effects.²⁰²

4. Concluding remarks and future perspectives

Catalytic processes are involved in more than 90% of the world chemical manufacturing processes. The activity and selectivity of a catalyst are often conditioned by its surface area, porosity, inertness, surface chemistry, purity, and cost effectiveness. However, the mechanical stability is also an important parameter to be considered for the possible recyclability of the catalyst. Besides these requirements, carbon materials additionally offer the possibility of easy tuning their surface chemistry, by using chemical and thermal post-modifications followed by functionalization, or by employing the appropriate synthetic approaches. Nevertheless, carbon supports also present some disadvantages: they can be easily gasified, which makes them difficult to use in high temperature hydrogenation and oxidation reactions, and their reproducibility can be poor, especially the activated carbon-based catalysts, since different batches of the same material can contain varying ash amounts.

Porous carbons, particularly ACs, are considered versatile and low cost catalysts and supports of the active phases with an application in a wide variety of organic transformations useful for the preparation of valuable products. The understanding of the surface chemistry of carbon materials is an important issue in the application of carbon as catalysts or even as supports for anchoring metal complexes or metal nanoparticles, between other active species.⁵ Additionally, functional groups over the surface of porous carbons can also hinder the migration of metal crystallites when acting as supports and, therefore, minimize their agglomeration and sintering. In fact, the performance of metal-supported catalysts depends mainly on one side on the metal loading and on the other side of its distribution and dispersion on the support, with the size of the metal particles a key factor in determining the catalyst performance. Therefore, the

synthesis of highly dispersed metal catalysts depends on the appropriate control of the surface chemistry.

The small-size limit of the supported metal particles is then a relevant aspect to be investigated in heterogeneous catalysis. In this context, the single-atom catalysts (SAC) are constituted by isolated metal atoms dispersed on supports.²⁰³ SACs offer great potential by giving rise to high activity and selectivity while showing well-defined and uniform single-atom dispersion. To this end, a strong metal–support interaction is the key to prevent aggregation of single atoms on the surface. Several supports such as metal oxides, metal surfaces, and graphene have been used for the preparation of SACs. In this sense, a few theoretical and experimental studies demonstrated that subnanometer-sized metal clusters can sometimes increase the catalytic activity or selectivity when compared with their nanometer-sized counterparts.²⁰⁴ Because of the great interest and potential of SACs in heterogeneous catalysis, the preparation and characterization of new SACs are considered an interesting challenge. When using SACs the catalytic performance may notably change because of the low-coordination environment, the quantum size effect, and improved metal–support interactions that maximize the metal efficiency. The development of SACs is then a new concept considered only the tip of the iceberg in heterogeneous catalysis and, interestingly, the understanding of those might be a new frontier in this field.

The nanocarbon-based catalysts are probably one of the most promising new scientific areas to develop the next-generation of catalysts.²⁰⁵ Their main disadvantage is the higher cost/performance ratio of these materials compared to that of standard heterogeneous catalysts or catalyst supports such as metal oxides (silica, alumina, *etc.*) or amorphous carbon ACs. It hinders the large-scale production thus slowing down the full breakthrough at the industrial level, although much progress has been made to improve preparative processes. The growing knowledge concerning their synthesis, the procedures to introduce surface functionalities (metallic or carbon based species), and the experimental or theoretical understanding of the defect nature and surface functional groups has completely changed the landscape and perspectives for the use of nanocarbons as conceptually new catalysts or catalyst supports. In this sense, the spectacular development of the characterization techniques, such as the microscopy and theoretical modeling, is clearly the key to understand in detail the surface chemistry and, therefore, to develop a rational design of nanocarbons for advanced catalytic applications.

Particularly, the remarkable features of CNFs and CNTs open new possibilities for catalysis, representing a new class of catalytic materials. However, some progress in this field is required. Thus, although knowledge from experimental and computational studies is growing, it is still missing a complete picture of how to show the relation between the presence of these surface functional groups and the characteristic nanodimension and nanoarchitecture of the nanocarbon. The stability of many of these functional groups is also still

an issue in comparison with “conventional” catalysts, as well as the possibility to maximize their concentration to improve the catalyst productivity. Nowadays their production processes are more controlled, but it is still very difficult to maintain homogeneity in all the features, and a better understanding of the growth processes and catalyst synthesis are needed. Moreover, critical aspects concerning standardization and toxicity²⁰⁶ should be addressed.

Acknowledgements

This work has been supported by MICINN (projects CTQ2011-27935 and CTM2014-56668-R).

Notes and references

- (a) P. Serp and J. L. Figueiredo, *Carbon Materials for Catalysis*, John Wiley & Sons, Hoboken, NJ, 2009; (b) F. Rodríguez-Reinoso, *Carbon*, 1998, **36**, 159; (c) A. J. Bird, in *Catalyst Supports and Supported Catalysts*, ed. A. B. Stiles, Butterworths, Boston, 1987.
- W. M. T. M. Reimerink, in *Adsorption and its Applications in Industry and Environmental Protection, vol I: Applications in Industry*, Elsevier, 1999, p. 751.
- (a) E. Pérez-Mayoral, V. Calvino-Casilda, M. Godino, A. J. López-Peinado and R. M. Martín-Aranda, in *Porous catalytic systems in the synthesis of bioactive heterocycles and related compounds Biologically. Relevant Heterocycles*, ed. G. Brahmachari, Elsevier, 2015, pp. 378–403; (b) E. Pérez-Mayoral, E. Soriano, R. M. Martín-Aranda and F. J. Maldonado-Hódar, in *Mesoporous Catalytic Materials and Fine Chemistry. Comprehensive Guide for Mesoporous Materials. Volume 1: Synthesis and Characterization*, ed. M. Aliofkhaeze, Nova Science Publishers, Inc., Series: Materials Science and Technologies, 2015; (c) L. R. Radovic and C. Sudhakar, in *Introduction to Carbon Technologies*, ed. H. Marsh, E. A. Heintz and F. Rodríguez-Reinoso, University of Alicante Press, Alicante, Spain, 1997.
- H. P. Boehm, *Carbon*, 1994, **32**, 759.
- (a) J. L. Figueiredo, *J. Mater. Chem. A*, 2013, **1**, 9351; (b) J. L. Figueiredo, M. Fernando and R. Pereira, *Catal. Today*, 2010, **150**, 2; (c) J. Lahaye, *Fuel*, 1998, **77**, 543.
- (a) E. Fuente, J. A. Menéndez, D. Suárez and M. A. Montes-Morán, *Langmuir*, 2003, **19**, 3505; (b) J. A. Menéndez, D. Suárez, E. Fuente and M. A. Montes-Morán, *Carbon*, 1999, **37**, 1002.
- H. Marsh and F. Rodríguez-Reinoso, *Activated carbon*, Elsevier, Oxford, 2006.
- D. S. Su, S. Perathoner and G. Centi, *Chem. Rev.*, 2013, **113**, 5782.
- E. H. L. Falcao and F. J. Wudl, *J. Chem. Technol. Biotechnol.*, 2007, **82**, 524.
- (a) L. R. Radovic and F. Rodríguez-Reinoso, in *Chemistry and Physics of Carbon*, ed. P. A. Thrower, Marcel Dekker, New York, 1997, vol. 25, pp. 243–358; (b) V. Calvino-Casilda, A. J. López-Peinado, C. J. Durán-Valle and R. M. Martín-Aranda, *Catal. Rev.: Sci. Eng.*, 2010, **52**, 325.

- 11 R. F. Heck and J. P. Jr. Nolley, *J. Org. Chem.*, 1972, **37**, 2320.
- 12 (a) D. S. Cameron, S. J. Cooper, I. L. Dodgson, B. Harrison and J. W. Jenkins, *Catal. Today*, 1990, **7**, 113; (b) E. Auer, A. Freund, J. Pietsch and T. Tacke, *Appl. Catal., A*, 1998, **173**, 259.
- 13 (a) B. M. Bhanage, M. Shirai and M. Arai, *J. Mol. Catal. A: Chem.*, 1999, **145**, 69; (b) F. Zhao, K. Murakami, M. Shirai and M. Arai, *J. Catal.*, 2000, **194**, 479.
- 14 R. G. Heidenreich, J. G. E. Krauter, J. Pietsch and K. Köhler, *J. Mol. Catal. A: Chem.*, 2002, **182–183**, 499.
- 15 S. S. Pröckl, W. Kleist and K. Köhler, *Tetrahedron*, 2005, **61**, 9855.
- 16 X. Fan, M. Gonzalez Manchon, K. Wilson, S. Tennison, A. Kozynchenko, A. A. Lapkin and P. K. Plucinski, *J. Catal.*, 2009, **267**, 114.
- 17 G. Marck, A. Villiger and R. Buchecker, *Tetrahedron Lett.*, 1994, **35**, 3277.
- 18 D. Gala, A. Stamford, J. Jenkins and M. Kugelman, *Org. Process Res. Dev.*, 1997, **1**, 163.
- 19 C. R. LeBlond, A. T. Andrews, Y. Sun and J. R. Sowa Jr., *Org. Lett.*, 2001, **3**, 1555.
- 20 (a) R. Narayanan, M. A. El-Sayed, R. Narayanan and M. A. El-Sayed, *J. Am. Chem. Soc.*, 2003, **125**, 8340; (b) R. Narayanan and M. A. El-Sayed, *J. Catal.*, 2005, **234**, 348.
- 21 S. S. Soomro, C. Röhlich and K. Köhler, *Adv. Synth. Catal.*, 2011, **353**, 767.
- 22 K. Köhler, R. G. Heidenreich, S. S. Soomro and S. S. Pröckl, *Adv. Synth. Catal.*, 2008, **350**, 2930.
- 23 S. Hermans, C. Diverchy, O. Demoulin, V. Dubois, E. M. Gaigneaux and M. Devillers, *J. Catal.*, 2006, **243**, 239.
- 24 L. B. Okhlopkova, *Appl. Catal., A*, 2009, **355**, 115.
- 25 O. M. Daniel, A. DeLaRiva, E. L. Kunkes, A. K. Datye, J. A. Dumesic and R. J. Davis, *ChemCatChem*, 2010, **2**, 1107.
- 26 K. M. Kaprielova, I. I. Ovchinnikov, O. A. Yakovina and A. S. Lisitsyn, *ChemCatChem*, 2013, **5**, 2015.
- 27 M. E. Halttunen, M. K. Niemelä, A. O. I. Krause and A. I. Vuori, *J. Mol. Catal. A: Chem.*, 1996, **109**, 209.
- 28 S. G. Wettstein, J. Q. Bond, D. Martin Alonso, H. N. Pham, A. K. Datye and J. A. Dumesic, *Appl. Catal., B*, 2012, **117–118**, 321.
- 29 Z. Zhao, H. Yang, Y. Li and X. Guo, *Green Chem.*, 2014, **16**, 1274.
- 30 E. Gallegos-Suárez, A. Guerrero-Ruiz, I. Rodriguez-Ramos and A. Arcoya, *Chem. Eng. J.*, 2015, **262**, 326.
- 31 W. B. Kim, E. D. Park, C. W. Lee and J. S. Lee, *J. Catal.*, 2003, **218**, 334.
- 32 W. B. Kim, E. D. Park and J. S. Lee, *Appl. Catal., A*, 2003, **242**, 335.
- 33 (a) R. A. Sheldon, I. W. C. E. Arends and A. Dijkstra, *Catal. Today*, 2000, **57**, 157; (b) R. A. Sheldon, I. W. C. E. Arends, I. G. J. ten Brink and A. Dijkstra, *Acc. Chem. Res.*, 2002, **35**, 774; (c) R. A. Sheldon and J. K. Kochi, *Metal-catalyzed oxidation of organic compounds*, Academic Press, New York, 1981.
- 34 Y. Chen, W. Chen, Q. Tang, Z. Guo, Y. Yang and F. Su, *Catal. Lett.*, 2011, **141**, 149.
- 35 J. Zhu, J. L. Faria, J. L. Figueiredo and A. Thomas, *Chem. – Eur. J.*, 2011, **17**, 7112.
- 36 *Mechanisms in Homogeneous and Heterogeneous Epoxidation Catalysis*, ed. S. Ted Oyama, 2008, Elsevier.
- 37 M.-L. Lin, K. Hara, Y. Okubo, M. Yanagi, H. Nambu and A. Fukuoka, *Catal. Commun.*, 2011, **12**, 1228.
- 38 A. Becker, *Inventory of Industrial Fluoro-Biochemicals*, Eyrolles, Paris, 1996.
- 39 J. Zhao, L. Ma, X.-L. Xu, F. Feng and X.-N. Li, *Chin. Chem. Lett.*, 2014, **25**, 1137.
- 40 M. Sugino, H. Shimada, T. Turuda, H. Miura, N. Ikenaga and T. Suzuki, *Appl. Catal., A*, 1995, **121**, 125.
- 41 K. Saito, K. Okuda, N. Ikenaga, T. Miyake and T. Suzuki, *J. Phys. Chem. A*, 2010, **114**, 3845.
- 42 (a) M. L. Granados, D. M. Alonso, I. Sadaba, R. Mariscal and P. Ocon, *Appl. Catal., B*, 2009, **89**, 265; (b) M. Kouzu, S. Yamanaka, J. Hidaka and M. Tsunomori, *Appl. Catal., A*, 2009, **355**, 94.
- 43 Y. Zu, G. Liu, Z. Wang, J. Shi, M. Zhang, W. Zhang and M. Jia, *Energy Fuels*, 2010, **24**, 3810.
- 44 G. Zhao, J. Shi, G. Liu, Y. Liu, Z. Wang, W. Zhang and M. Jia, *J. Mol. Catal. A: Chem.*, 2010, **327**, 32.
- 45 M. Godino-Ojer, A. J. López-Peinado, R. M. Martín-Aranda, J. Przepiórski, E. Pérez-Mayoral and E. Soriano, *ChemCatChem*, 2014, **6**, 3440.
- 46 E. Soriano, E. Pérez-Mayoral, M. C. Carreiras and J. Marco-Contelles, *Chem. Rev.*, 2009, **109**, 2671.
- 47 V. Calvino-Casilda, A. J. López-Peinado, J. L. G. Fierro and R. M. Martín-Aranda, *Appl. Catal., A*, 2003, **240**, 287.
- 48 V. Calvino-Casilda, R. M. Martín-Aranda and A. J. López-Peinado, *Catal. Lett.*, 2009, **129**, 281.
- 49 V. Calvino-Casilda, R. M. Martín-Aranda and A. J. López-Peinado, *Environ. Prog. Sustainable Energy*, 2011, **30**, 469.
- 50 (a) V. Calvino-Casilda, A. J. López-Peinado, R. M. Martín-Aranda, S. Ferrera-Escudero and C. J. Durán-Valle, *Carbon*, 2004, **42**, 1363; (b) S. Ferrera-Escudero, E. Perozo-Rondón, V. Calvino-Casilda, B. Casal, R. M. Martín-Aranda, A. J. López-Peinado and C. J. Durán-Valle, *Appl. Catal., A*, 2010, **378**, 26.
- 51 (a) V. Calvino Casilda, E. Pérez-Mayoral, M. A. Bañares and E. Lozano Diz, *Chem. Eng. J.*, 2010, **161**, 371; (b) V. Calvino Casilda and M. A. Bañares, *Catal. Today*, 2012, **187**, 191.
- 52 V. Calvino-Casilda, R. M. Martín-Aranda and A. J. López-Peinado, *Appl. Catal., A*, 2011, **398**, 73.
- 53 C. J. Durán-Valle, I. M. Fonseca, V. Calvino-Casilda, M. Picallo, A. J. López-Peinado and R. M. Martín-Aranda, *Catal. Today*, 2005, **107–108**, 500.
- 54 A. R. Keterling, A. S. Lisitsyn, V. A. Likholobov, A. A. Gall and E. S. Trachum, *Kinet. Catal.*, 1990, **31**, 1273.
- 55 (a) S. Bischoff, A. Weigt, H. Miessner and B. Lucke, *Energy Fuels*, 1996, **10**, 520; (b) S. Bischoff, A. Weigt, H. Miessner and B. Lucke, *J. Mol. Catal. A: Chem.*, 1996, **107**, 339.
- 56 P. C. L'Argentiere, M. E. Quiroga, D. A. Liprandi, E. A. Cagnola, M. C. Román-Martínez, J. A. Díaz-Auñón and C. Salinas-Martínez de Lecea, *Catal. Lett.*, 2003, **87**, 97.
- 57 M. Quiroga, D. Liprandi, P. L'Argentiere and E. Cagnola, *J. Chem. Technol. Biotechnol.*, 2005, **80**, 158.

- 58 (a) L. Lemus-Yegres, I. Such-Basáñez, C. Salinas-Martínez de Lecea, P. Serp and M. C. Román-Martínez, *Carbon*, 2006, **44**, 587; (b) L. J. Lemus-Yegres, M. C. Román-Martínez, I. Such-Basáñez and C. Salinas-Martínez de Lecea, *Microporous Mesoporous Mater.*, 2008, **109**, 305.
- 59 L. J. Lemus-yegres, I. Such-Basáñez, M. C. Román-Martínez and C. Salinas-Martínez de Lecea, *Appl. Catal., A*, 2007, **331**, 26–33.
- 60 M. Pérez-Cadenas, L. J. Lemus-Yegres, M. C. Román-Martínez and C. Salinas-Martínez de Lecea, *Appl. Catal., A*, 2011, **402**, 132.
- 61 L. Wachowski, W. Skupinski and M. Hofman, *Appl. Catal., A*, 2006, **303**, 230.
- 62 (a) A. R. Silva, J. Vital, J. L. Figueiredo, C. Freire and B. Castro, *New J. Chem.*, 2003, **27**, 1511; (b) A. R. Silva, J. L. Figueiredo, C. Freire and B. Castro, *Microporous Mesoporous Mater.*, 2004, **68**, 83.
- 63 A. R. Silva, C. Freire, B. Castro, M. M. A. Freitas and J. L. Figueiredo, *Microporous Mesoporous Mater.*, 2001, **46**, 211.
- 64 A. R. Silva, V. Budarin, J. H. Clark, B. de Castro and C. Freire, *Carbon*, 2005, **43**, 2096.
- 65 F. Maia, R. Silva, B. Jarrais, A. R. Silva, C. Freire, M. F. R. Pereira and J. L. Figueiredo, *J. Colloid Interface Sci.*, 2008, **328**, 314.
- 66 F. C. C. Moura, E. N. dos Santos, R. M. Lago, M. D. Vargas and M. H. Araujo, *J. Mol. Catal. A: Chem.*, 2005, **226**, 243.
- 67 M. Peixoto de Almeida, L. M. D. R. S. Martins, S. A. C. Carabineiro, T. Lauterbach, F. Rominger, A. S. K. Hashmi, A. J. L. Pombeiro and J. L. Figueiredo, *Catal. Sci. Technol.*, 2013, **3**, 3056.
- 68 A. R. Silva and J. Botelho, *J. Mol. Catal. A: Chem.*, 2014, **381**, 171.
- 69 Y. Izumi and K. Urabe, *Chem. Lett.*, 1981, 663.
- 70 M. E. Chimienti, L. R. Pizzio, C. V. Cáceres and M. N. Blanc, *Appl. Catal., A*, 2001, **208**, 7.
- 71 L. R. Pizzio, P. G. Vázquez, C. V. Cáceres, M. N. Blanco, E. N. Alesso, M. I. Erlich, R. Torviso, L. Finkielstein, B. Lantaño, G. Y. Moltrasio and J. M. Aguirre, *Catal. Lett.*, 2004, **93**, 1.
- 72 F. Lefebvre, P. DuPont and A. Auroux, *React. Kinet. Catal. Lett.*, 1995, **55**, 3.
- 73 P. DuPont, J. C. Vadrine, E. Paumard, G. Hecquet and F. Lefebvre, *Appl. Catal., A*, 1995, **129**, 217.
- 74 P. DuPont and F. Lefebvre, *J. Mol. Catal. A: Chem.*, 1996, **114**, 299.
- 75 E. Rafiee, F. Paknezhad, S. Shahebrahimi, M. Joshaghani, S. Eavani and S. Rashidzadeh, *J. Mol. Catal. A: Chem.*, 2008, **282**, 92.
- 76 E. Rafiee, S. Eavani, S. Rashidzadeh and M. Joshaghani, *Inorg. Chim. Acta*, 2009, **362**, 3555.
- 77 E. Rafiee, H. Mahdavi, S. Eavani, M. Joshaghani and F. Shiri, *Appl. Catal., A*, 2009, **352**, 202.
- 78 P. Ferreira, I. M. Fonseca, A. M. Ramos, J. Vital and J. E. Castanheiro, *Catal. Commun.*, 2011, **12**, 573.
- 79 J. Alcañiz-Monge, G. Trautwein and J. P. Marco-Lozar, *Appl. Catal., A*, 2013, **468**, 432.
- 80 (a) A. S. Badday, A. Zuhairi Abdullah and K.-T. Lee, *Renewable Energy*, 2013, **50**, 427; (b) A. S. Badday, A. Zuhairi Abdullah and K.-T. Lee, *Renewable Energy*, 2014, **62**, 10.
- 81 M. Haruta, *Gold Bull.*, 2004, **37**, 27.
- 82 A. Abad, A. Corma and H. García, *Top. Catal.*, 2007, **44**, 239.
- 83 W. Wittanadecha, N. Laosiripojana, A. Ketcong, N. Ningnuek, P. Praserthdam, J. R. Monnier and S. Assabumrungrat, *Appl. Catal., A*, 2014, **475**, 292.
- 84 J. Xu, J. Zhao, J. Xu, T. Zhang, X. Li, X. Di, J. Ni, J. Wang and J. Cen, *Ind. Eng. Chem. Res.*, 2014, **53**, 14272.
- 85 C. Huang, M. Zhu, L. Kang, X. Li and B. Dai, *Chem. Eng. J.*, 2014, **242**, 69.
- 86 H. Zhang, B. Dai, W. Li, X. Wang, J. Zhang, M. Zhu and J. Gu, *J. Catal.*, 2014, **316**, 141.
- 87 M. Bonarowska, Z. Kaszkur, D. Łomot, M. Rawski and Z. Karpinski, *Appl. Catal., B*, 2015, **162**, 45.
- 88 H. Okatsu, N. Kinoshita, T. Akita, T. Ishida and M. Haruta, *Appl. Catal., A*, 2009, **369**, 8.
- 89 S. Hermans, A. Deffernez and M. Devillers, *Catal. Today*, 2010, **157**, 77.
- 90 (a) S. Demirel, K. Lehnert, M. Lucas and P. Claus, *Appl. Catal., B*, 2007, **70**, 637; (b) E. G. Rodrigues, M. F. R. Pereira, J. J. Delgado, X. Chen and J. J. M. Órfão, *Catal. Commun.*, 2011, **16**, 64.
- 91 (a) E. G. Rodrigues, M. F. R. Pereira, X. Chen, J. J. Delgado and J. J. M. Órfão, *J. Catal.*, 2011, **281**, 119; (b) E. G. Rodrigues, S. A. C. Carabineiro, X. Chen, J. J. Delgado, J. L. Figueiredo, M. F. R. Pereira and J. J. M. Orfao, *Catal. Lett.*, 2011, **141**, 420.
- 92 (a) I. Sobczak, K. Jagodzinska and M. Ziolk, *Catal. Today*, 2010, **158**, 121; (b) S. Gil, M. Marchena, L. Sánchez-Silva, A. Romero, P. Sánchez and J. L. Valverde, *Chem. Eng. J.*, 2011, **178**, 423.
- 93 C. M. Domínguez, A. Quintanilla, J. A. Casas and J. J. Rodríguez, *Chem. Eng. J.*, 2014, **253**, 486.
- 94 (a) D. Wang, A. Villa, F. Porta, L. Prati and D. Su, *J. Phys. Chem. C*, 2008, **112**, 8617; (b) C. E. Chan-Thaw, S. Campisi, D. Wang, L. Prati and A. Villa, *Catalysts*, 2015, **5**, 131.
- 95 N. Dimitratos, A. Villa and L. Prati, *Catal. Lett.*, 2009, **133**, 334.
- 96 T. Szumelda, A. Drelinkiewicz, R. Kosydar and J. Gurgul, *Appl. Catal., A*, 2014, **487**, 1.
- 97 N. M. Julkapli and S. Bagheri, *Int. J. Hydrogen Energy*, 2015, **40**, 948.
- 98 X. Xie, J. Long, J. Xu, L. Chen, Y. Wang, Z. Zhanga and X. Wang, *RSC Adv.*, 2012, **2**, 12438.
- 99 C. Su, R. Tandiana, J. Balapanuru, W. Tang, K. Pareek, C. T. Nai, T. Hayashi and K. P. Loh, *J. Am. Chem. Soc.*, 2015, **137**, 685.
- 100 D. Verma, S. Verma, A. K. Sinha and S. L. Jain, *ChemPlusChem*, 2013, **78**, 860.
- 101 M. Blanco, P. Álvarez, C. Blanco, M. V. Jiménez, J. Fernández-Tornos, J. J. Pérez-Torrente, L. A. Oro and R. Menéndez, *Carbon*, 2015, **83**, 21.
- 102 S. Sabater, J. A. Mata and E. Peris, *ACS Catal.*, 2014, **4**, 2038.

- 103 S. Moussa, A. R. Siamaki, B. F. Gupton and M. S. El-Shall, *ACS Catal.*, 2012, 2, 145.
- 104 S. Santra, P. K. Hota, R. Bhattacharyya, P. Bera, P. Ghosh and S. K. Mandal, *ACS Catal.*, 2013, 3, 2776.
- 105 A. Shaabani and M. Mahyari, *J. Mater. Chem. A*, 2013, 1, 9303.
- 106 J. Liu, X. Huo, T. Li, Z. Yang, P. Xi, Z. Wang and B. Wan, *Chem. – Eur. J.*, 2014, 20, 11549.
- 107 A. Primo, I. Esteve-Adell, J. F. Blandez, A. Dhakshinamoorthy, M. Álvaro, N. Candu, S. M. Coman, V. I. Parvulescu and H. García, *Nat. Commun.*, 2015, 8561, DOI: 10.1038/ncomms9561.
- 108 Y. Hernandez, V. Nicolosi, M. Lotya, F. M. Blighe, Z. Sun, S. De, I. T. McGovern, B. Holland, M. Byrne, Y. K. Gun'Ko, J. J. Boland, P. Niraj, G. Duesberg, S. Krishnamurthy, R. Goodhue, J. Hutchison, V. Scardaci, A. C. Ferrari and J. N. Coleman, *Nat. Nanotechnol.*, 2008, 3, 563.
- 109 P. Serp, M. Corrias and P. Kalck, *Appl. Catal., A*, 2003, 253, 337.
- 110 N. M. Rodriguez, A. Chambers and R. T. K. Baker, *Langmuir*, 1995, 11, 3862.
- 111 H.-Y. Cheng, Y.-A. Zhu, Z.-J. Sui, X.-G. Zhou and D. Chen, *Carbon*, 2012, 50, 4359.
- 112 P. Morgan, in *Carbon fibers and their composites*, CRC Press (Taylor & Francis Group), Boca Raton, 2005.
- 113 J. Zhu, A. Holmen and De Chen, *ChemCatChem*, 2013, 5, 378.
- 114 N. M. Rodriguez, M.-S. Kim and R. T. K. Baker, *J. Phys. Chem.*, 1994, 98, 13108.
- 115 (a) J. Huang, Y. Liu and T. You, *Anal. Methods*, 2010, 2, 202; (b) M. Endo, Y. A. Kim, T. Hayashi, K. Nishimura, T. Matusita, K. Miyashita and M. S. Dresselhaus, *Carbon*, 2001, 39, 1287.
- 116 K. P. de Jong and J. W. Geus, *Catal. Rev.: Sci. Eng.*, 2000, 42, 481.
- 117 N. Saito, K. Aoki, Y. Usui, M. Shimizu, K. Hara, N. Narita, N. Ogihara, K. Nakamura, N. Ishigaki, H. Kato, H. Haniu, S. Taruta, Y. A. Kim and M. Endo, *Chem. Soc. Rev.*, 2011, 40, 3824.
- 118 (a) H. J. Dai, *Surf. Sci.*, 2002, 500, 218; (b) P. Serp and E. Castillejos, *ChemCatChem*, 2010, 2, 41; (c) D. Tasis, N. Tagmatarchis, A. Bianco and M. Prato, *Chem. Rev.*, 2006, 106, 1105; (d) G. G. Wildgoose, C. E. Banks and R. G. Compton, *Small*, 2006, 2, 182.
- 119 Z. X. Yu, D. Chen, B. Totdal and A. Holmen, *J. Phys. Chem. B*, 2005, 109, 6096.
- 120 V. Georgakilas, J. A. Perman, J. Tucek and R. Zboril, *Chem. Rev.*, 2015, 115, 4744.
- 121 (a) P. Serp, in *Carbon materials for catalysis*, ed. P. Serp and J. L. Figueiredo, Wiley, 2009, ch. 9; (b) P. Serp and B. Machado, in *Nanostructured Carbon Materials for Catalysis*, RSC Catalysis Series, 2015, ch. 7.
- 122 C. Park and R. T. K. Baker, *J. Phys. Chem. B*, 1998, 102, 5168.
- 123 T. G. Ros, D. E. Keller, A. J. van Dillen, J. W. Geus and D. C. Koningsberger, *J. Catal.*, 2002, 211, 85.
- 124 M. Takasaki, Y. Motoyama, K. Higashi, S.-H. Yoon, I. Mochida and H. Nagashima, *Chem. – Asian J.*, 2007, 2, 1524.
- 125 C. Park and M. A. Keane, *J. Colloid Interface Sci.*, 2003, 266, 183.
- 126 F. Salman, C. Park and R. T. K. Baker, *Catal. Today*, 1999, 53, 385.
- 127 C. Pham-Huu, N. Keller, G. Ehret, L. J. Charbonniere, R. Ziessel and M. J. Ledoux, *J. Mol. Catal. A: Chem.*, 2001, 170, 155.
- 128 M. L. Toebes, F. F. Prinsloo, J. H. Bitter, A. J. van Dillen and K. P. de Jong, *J. Catal.*, 2003, 214, 78.
- 129 (a) P. Li, Y. L. Huang, D. Chen, J. Zhu, T. J. Zhao and X. G. Zhou, *Catal. Commun.*, 2009, 10, 815; (b) Q. Zhou, P. Li, X. Wang, X. Zhou, D. Yang and De Chen, *Mat. Chem. Phys.*, 2011, 126, 41.
- 130 H.-B. Zhang, X. Dong, G.-D. Lin, X.-L. Liang and H.-Y. Lia, *Chem. Commun.*, 2005, 5094.
- 131 R. Gao, C. D. Tan and R. T. K. Baker, *Catal. Today*, 2001, 65, 19.
- 132 C. Liang, Z. Li, J. Qiu and C. Li, *J. Catal.*, 2002, 211, 278.
- 133 L. Zhao, J. H. Zhou, Z. J. Sui and X. G. Zhou, *Chem. Eng. Sci.*, 2010, 65, 30.
- 134 S. Van de Vyver, J. Geboers, W. Schutyser, M. Dusselier, P. Eloy, E. Dornez, J. W. Seo, C. M. Courtin, E. M. Gaigneaux, P. A. Jacobs and B. F. Sels, *ChemSusChem*, 2012, 5, 1549.
- 135 M. Zhang, R. Nie, L. Wang, J. Shi, W. Du and Z. Hou, *Catal. Commun.*, 2015, 59, 5.
- 136 T. van Haasterecht, T. W. van Deelen, K. P. de Jong and J. H. Bitter, *Catal. Sci. Technol.*, 2014, 4, 2353.
- 137 X. Fu, H. Yu, F. Peng, Hongjuan Wang and Y. Qian, *Appl. Catal., A*, 2007, 321, 190.
- 138 R. T. K. Baker, N. Rodriguez, Á. Mastalir, U. Wild, R. Schlögl, A. Wootsch and Z. Paál, *J. Phys. Chem. B*, 2004, 108, 14348.
- 139 A. M. Frey, J. H. Bitter and K. P. de Jong, *ChemCatChem*, 2011, 3, 1193.
- 140 A. W. A. M. van der Heijden, S. G. Podkolzin, M. E. Jones, J. H. Bitter and B. M. Weckhuysen, *Angew. Chem., Int. Ed.*, 2008, 47, 5002.
- 141 J. Zhu, J. Zhou, T. Zhao, X. Zhou, D. Chen and W. Yuan, *Appl. Catal., A*, 2009, 352, 243.
- 142 R. Vieira, D. Bastos-Netto, M.-J. Ledoux and C. Pham-Huu, *Appl. Catal., A*, 2005, 279, 35.
- 143 F. Winter, V. Koot, A. J. van Dillen, J. W. Geus and K. P. de Jong, *J. Catal.*, 2005, 236, 91.
- 144 T. Belin and F. Epron, *Mater. Sci. Eng., B*, 2005, 119, 105.
- 145 L. R. Radovic and B. Bockrath, *J. Am. Chem. Soc.*, 2005, 127, 5917.
- 146 S. Iijima, *Nature*, 1991, 354, 56.
- 147 J. Y. Huang, S. Chen, Z. Q. Wang, K. Kempa, Y. M. Wang, S. H. Jo, G. Chen, M. S. Dresselhaus and Z. F. Ren, *Nature*, 2006, 439, 281.
- 148 F. Ding, K. Jiao, Y. Lin and B. I. Yakobson, *Nano Lett.*, 2007, 7, 681.
- 149 D. S. Bethune, C. H. Klang, M. S. D. Vries and J. Gorman, *Nature*, 1993, 363, 605.

- 150 H. Dai, *Acc. Chem. Res.*, 2002, 35, 1035.
- 151 S. Agnihotri, J. P. B. Mota, M. R. Abadi and M. J. Rood, *Langmuir*, 2005, 21, 896.
- 152 F. Wang, L. Lang, B. Li, W. Liu, X. Li and Z. Xu, *Mater. Lett.*, 2010, 64, 86.
- 153 (a) H. J. Dai, *Surf. Sci.*, 2002, 500, 218; (b) M. Terrones, *Int. Mater. Rev.*, 2004, 49, 325; (c) A. Mostofizadeh, Y. Li, B. Song and Y. Huang, *J. Nanomater.*, 2011, 685081; (d) M. Terrones, A. G. Souza and A. M. Rao, in *Carbon Nanotubes*, 2008, vol. 111, pp. 531–566; (e) J. Prasek, J. Drbohlavova, J. Chomoucka, J. Hubalek, O. Jasek, V. Adam and R. Kizek, *J. Mater. Chem.*, 2011, 21, 15872; (f) P. J. F. Harris, *Carbon Nanotube Science. Synthesis, Properties and Applications*, Cambridge University, 2011; (g) *Carbon Nanotubes. Synthesis, Structure, Properties, and Applications*, *Top. Appl. Phys.*, ed. M. S. Dresselhaus, G. Dresselhaus and P. Avouris, 2015.
- 154 (a) V. Georgakilas, M. Otyepka, A. B. Bourlinos, V. Chandra, N. Kim, K. C. Kemp, P. Hobza, R. Zboril and K. S. Kim, *Chem. Rev.*, 2012, 112, 6156; (b) V. Georgakilas, D. Gournis, V. Tzitzios, L. Pasquato, D. M. Guldie and M. Prato, *J. Mater. Chem.*, 2007, 17, 2679; (c) G. G. Wildgoose, C. E. Banks and R. G. Compton, *Small*, 2006, 2, 182.
- 155 K. J. Kong, Y. Choi, B. H. Ryu, J. O. Lee and H. Chang, *Mater. Sci. Eng., C*, 2006, 26, 1207.
- 156 L. M. Ombaka, P. Ndungu and V. O. Nyamori, *Catal. Today*, 2013, 217, 65.
- 157 N. Karousis and N. Tagmatarchis, *Chem. Rev.*, 2010, 110, 5366.
- 158 C. Yonghai, Y. Hao, T. Jun, P. Feng, W. Hongjuan, L. Jing, Z. Wenxu and W. Ning-Bew, *Carbon*, 2013, 57, 433.
- 159 (a) Y. Jiang, J. Zhang, Y.-H. Qin, D.-F. Niu, X.-S. Zhang, L. Niu, X.-G. Zhou, T.-H. Lu and W.-K. Yuan, *J. Power Sources*, 2011, 196, 9356; (b) R. I. Jafri, N. Rajalakshmi and S. Ramaprabhu, *J. Mater. Chem.*, 2010, 20, 7114.
- 160 Y. Shao, J. Sui, G. Yin and Y. Gao, *Appl. Catal., B*, 2008, 79, 89.
- 161 Y. Motoyama, Y. Lee, K. Tsuji, S.-H. Yoon, I. Mochida and H. Nagashima, *ChemCatChem*, 2011, 3, 1578.
- 162 (a) H. Wang, T. Maiyalagan and X. Wang, *ACS Catal.*, 2012, 2, 781; (b) G. Liu, X. Li, J.-W. Lee and B. N. Popov, *Catal. Sci. Technol.*, 2011, 1, 207; (c) H. P. Boehm, *Catalytic Properties of Nitrogen-Containing Carbons*, in *Carbon Materials for Catalysis*, ed. P. Serp and J. L. Figueiredo, John Wiley & Sons, New York, 2008, p. 219.
- 163 F. R. García-García, J. Alvarez-Rodríguez, I. Rodríguez-Ramos and A. Guerrero-Ruiz, *Carbon*, 2010, 48, 267.
- 164 W. An and C. H. Turner, *J. Phys. Chem. C*, 2009, 113, 7069.
- 165 L. M. Ombaka, P. G. Ndungu and V. O. Nyamori, *RSC Adv.*, 2015, 5, 109.
- 166 (a) J. Z. Chen, W. Zhang, L. M. Chen, L. L. Ma, H. Gao and T. J. Wang, *ChemPlusChem*, 2013, 78, 142; (b) A. B. Chen, Y. L. Li, J. Z. Chen, G. Y. Zhao, L. L. Ma and Y. F. Yu, *ChemPlusChem*, 2013, 78, 1370.
- 167 J. Chen, J. Zhong, Y. Guo and L. Chen, *RSC Adv.*, 2015, 5, 5933.
- 168 Z. Sun, H. Zhang, Y. Zhao, C. Huang, R. Tao, Z. Liu and Z. Wu, *Langmuir*, 2011, 27, 6244.
- 169 A. Jung, A. Jess, T. Schubert and W. Schuetz, *Appl. Catal., A*, 2009, 362, 95.
- 170 (a) C. H. Li, Z. X. Yu, K. F. Yao, S. F. Ji and J. Liang, *J. Mol. Catal. A: Chem.*, 2005, 226, 101; (b) Z. Y. Sun, Y. F. Zhao, Y. Xie, R. T. Tao, H. Y. Zhang, C. L. Huang and Z. M. Liu, *Green Chem.*, 2010, 12, 1007.
- 171 V. Lordi, N. Yao and J. Wei, *Chem. Mater.*, 2001, 13, 733.
- 172 (a) V. Brotons, B. Coq and J. M. Planeix, *J. Mol. Catal.*, 1997, 116, 397; (b) C. Wang, J. S. Qiu, C. H. Liang, L. Xing and X. M. Yang, *Catal. Commun.*, 2008, 9, 1749.
- 173 H. Vu, F. Goncalves, R. Philippe, E. Lamouroux, M. Corrias, Y. Kihn, D. Plee, P. Kalck and P. Serp, *J. Catal.*, 2006, 240, 18.
- 174 (a) R. Giordano, P. Serp, P. Kalck, Y. Kihn, J. Schreiber, C. Marhic and J.-L. Duvail, *Eur. J. Inorg. Chem.*, 2003, 610; (b) B. F. Machado, H. T. Gomes, P. Serp, P. Kalck and J. L. Faria, *ChemCatChem*, 2010, 2, 190.
- 175 Z.-J. Liu, Z. Xu, Z.-Y. Yuan, D. Lu, W. Chen and W. Zhou, *Catal. Lett.*, 2001, 72, 203.
- 176 R. Rao, Q. Zhang, H. Liu, H. Yang, Q. Ling, M. Yang, A. Zhang and W. Chen, *J. Mol. Catal. A: Chem.*, 2012, 363–364, 283.
- 177 Y. Zhang, H.-B. Zhang, G.-D. Lin, P. Chen, Y.-Z. Yuan and K. R. Tsai, *Appl. Catal., A*, 1999, 187, 213.
- 178 H.-B. Chen, J.-D. Lin, Y. Cai, X.-Y. Wang, J. Yi, J. Wang, G. Wei, Y.-Z. Lin and D. W. Liao, *Appl. Surf. Sci.*, 2001, 180, 328.
- 179 H. Wang, L. Zhu, S. Peng, F. Peng, H. Yu and J. Yang, *Renewable Energy*, 2012, 37, 192.
- 180 T. Hou, L. Yuan, T. Ye, L. Gong, J. Tu, M. Yamamoto, Y. Torimoto and Q. Li, *Int. J. Hydrogen Energy*, 2009, 34, 9095.
- 181 E. G. Rodrigues, S. A. C. Carabineiro, J. J. Delgado, X. Chen, M. F. R. Pereira and J. J. M. Orfao, *J. Catal.*, 2012, 285, 83.
- 182 E. F. Mai, M. A. Machado, T. E. Davies, J. A. López-Sánchez and V. Teixeira da Silva, *Green Chem.*, 2014, 16, 4092.
- 183 M. S. Saha, R. Li and X. Sun, *J. Power Sources*, 2008, 177, 314.
- 184 H. T. Tan, Y. Chen, C. Zhou, X. Jia, J. Zhu, J. Chen, X. Rui, Q. Yan and Y. Yang, *Appl. Catal., B*, 2012, 119–120, 166.
- 185 M. Nooraiepour, M. Moghadam, S. Tangestaninejad, V. Mirkhani, I. Mohammadpoor-Baltork and N. Iravani, *J. Coord. Chem.*, 2012, 65, 226.
- 186 G. Ovejero, J. L. Sotelo, M. D. Romero, A. Rodriguez, M. A. Ocana, G. Rodriguez and J. Garcia, *Ind. Eng. Chem. Res.*, 2006, 45, 2206.
- 187 J. Safari and S. Gandomi-Ravandi, *J. Mol. Struct.*, 2014, 1072, 173.
- 188 B. Cornelio, G. A. Rance, M. Laronze-Cochard, A. Fontana, J. Sapi and A. N. Khlobystov, *J. Mater. Chem. A*, 2013, 1, 8737.
- 189 J. Y. Kim, Y. Jo, S. Lee and H. C. Choi, *Tetrahedron Lett.*, 2009, 50, 6290.
- 190 X. Pan and X. Bao, *Chem. Commun.*, 2008, 6271.
- 191 X. Pan and X. Bao, *Acc. Chem. Res.*, 2011, 44, 553–562.

- 192 S. Guo, X. Pan, H. Gao, Z. Yang, J. Zhao and X. Bao, *Chem. – Eur. J.*, 2010, **16**, 5379.
- 193 X. Duan, J. Zhou, G. Qian, P. Li, X. Zhou and D. Chen, *Chin. J. Catal.*, 2010, **31**, 979.
- 194 X.-F. Guo, D.-Y. Jang, H.-G. Jang and G.-J. Kim, *Catal. Today*, 2012, **186**, 109.
- 195 S. Mao, G. H. Lu and J. H. Chen, *J. Mater. Chem. A*, 2014, **2**, 5573.
- 196 O. Ito and F. E. C. S. D'Souza, *ECS J. Solid State Sci. Technol.*, 2013, **2**, M3063.
- 197 K. Dirian, M. A. Herranz, G. Katsukis, J. Malig, L. Rodríguez-Perez, C. Romero-Nieto, V. Strauss, N. Martin and D. M. Guldi, *Chem. Sci.*, 2013, **4**, 4335.
- 198 Q. H. Wang, D. O. Bellisario, L. W. Drahushuk, R. M. Jain, S. Kruss, M. P. Landry, S. G. Mahajan, S. F. E. Shimizu, Z. W. Ulissi and M. S. Strano, *Chem. Mater.*, 2014, **26**, 172.
- 199 M. B. Bryning, D. E. Millie, M. F. Islam, L. A. Hough, J. M. Kikkawa and A. G. Yodh, *Adv. Mater.*, 2007, **19**, 661.
- 200 M. A. Worsley, S. O. Kucheyev, J. D. Kuntz, T. Y. Olson, T. Y. J. Han, A. V. Hamza, J. H. Satcher and T. F. Baumann, *Chem. Mater.*, 2011, **23**, 3054.
- 201 M. C. Gutierrez, M. J. Hortigüela, J. M. Amarilla, R. Jiménez, M. L. Ferrer and F. del Monte, *J. Phys. Chem. C*, 2007, **111**, 5557.
- 202 Z. Li, Z. Liu, H. Sun and C. Gao, *Chem. Rev.*, 2015, **115**, 7046.
- 203 X.-F. Yang, A. Wang, B. Qiao, J. Li, J. Liu and T. Zhang, *Acc. Chem. Res.*, 2013, **46**, 1740.
- 204 A. A. Herzing, C. J. Kiely, A. F. Carley, P. Landon and G. J. Hutchings, *Science*, 2008, **321**, 1331.
- 205 M. Melchionna, S. Marchesan, M. Prato and P. Fornasiero, *Catal. Sci. Technol.*, 2015, **5**, 3859.
- 206 (a) L. Horváth, A. Magrez, B. Schwaller and L. Forró, Toxicity Study of Nanofibers, in *Supramolecular Structure and Function 10*, ed. J. Brnjas-Kraljevi and G. Pifat-Mrzljak, 2011, ch. 9, pp. 133–149; (b) Y. Liu, Y. Zhao, B. Sun and C. Chen, *Acc. Chem. Res.*, 2013, **46**, 702.